รายงานวิจัยฉบับสมบูรณ์

โครงการ: การศึกษาหน้าที่ของยีนที่สำคัญและกลไกการทำงานของยาต้านมาลาเรีย โดยควบคุมการแสดงออกของยีนด้วยระบบไรโบไซม์ในเชื้อปรสิตพลาสโมเดียมฟาลซิปารัม

Exploration of essential gene function and antimalarial mode of action by ribozyme-mediated attenuation of gene activity in the human malaria parasite *Plasmodium falciparum*

โดย นายฟิลิป เจมส์ ชอว์ และคณะ

ศูนย์พันธุวิศวกรรมและเทคโนโลยีชีวภาพแห่งชาติ

สำนักงานพัฒนาวิทยาศาสตร์และเทคโนโลยีแห่งชาติ

โครงการเสร็จสิ้นเมื่อ เดือนมิถุนายน ปี พ.ศ. 2560

สัญญาเลขที่ RSA5780007

รายงานวิจัยฉบับสมบูรณ์

โครงการ: การศึกษาหน้าที่ของยีนที่สำคัญและกลไกการทำงานของยาต้านมาลาเรีย โดยควบคุมการแสดงออกของยีนด้วยระบบไรโบไซม์ในเชื้อปรสิตพลาสโมเดียมฟาลซิปารัม

Exploration of essential gene function and antimalarial mode of action by ribozyme-mediated attenuation of gene activity in the human malaria parasite *Plasmodium falciparum*

หัวหน้าโครงการวิจัยผู้รับทุน: นายฟิลิป เจมส์ ชอว์

ศูนย์พันธุวิศวกรรมและเทคโนโลยีชีวภาพแห่งชาติ

สำนักงานพัฒนาวิทยาศาสตร์และเทคโนโลยีแห่งชาติ

สนับสนุนโดยสำนักงานกองทุนสนับสนุนการวิจัย

และศูนย์พันธุวิศวกรรมและเทคโนโลยีชีวภาพแห่งชาติ

Abstract

Control, and ultimately eradication of malaria will require a variety of new antimalarial drugs. Progress towards this goal is hampered by inadequate reverse-genetic tools for identifying drug targets and antimalarial mode of action. The aim of the project was to refine the *glmS* ribozyme reverse genetic tool developed in our laboratory. This tool can be used to attenuate the expression of essential genes, including drug targets. Clonal integrant transgenic parasites were established for the dihydrofolate reductase-thymidylate synthase (DHFR-TS) and deoxyhypusine synthase (DHS) genes. For the DHS gene, transgenic parasites with both the active *glmS* ribozyme and the inactive M9 variant as a control were obtained. Up to ten-fold attenuation of target gene expression was observed in transgenic parasites carrying insertion of the active *glmS* ribozyme when treated with D-glucosamine (GlcN). In contrast, no significant attenuation of DHS expression was observed in DHS modified parasites with the M9 variant inactive ribozyme. Attenuation of DHFR-TS and DHS expression in transgenic parasites led to a significant growth defect, thus validating these genes as essential. A chemogenomic profiling method was developed in which growth inhibition of antimalarial compounds was quantified under normal and gene-attenuated conditions in the transgenic parasites. The mode of action of antimalarial compounds was manifested as increased sensitivity to growth inhibition under gene-attenuated conditions. Two novel inhibitors of DHFR-TS were identified from screening the Malaria Box compound library of 400 compounds. Using the same method, the DHS gene was identified as the target of N1-guanyl-1,7-diaminoheptane, a known inhibitor of DHS enzymes in other organisms. In conclusion, a novel antimalarial target (the DHS gene) and the mode of action of two novel antimalarial compounds were identified. Future studies utilizing the tools and methods developed from this study could lead to identification of more drug targets and greater understanding of antimalarial mode of action.

บทคัดย่อ

ในปัจจุบัน เป้าหมายในการควบคุมอัตราการเกิดโรคมาลาเรียหรือการทำให้โรคมาลาเรียหมดไปนั้น ยังต้องอาศัยการพัฒนายาต้านมาลาเรียใหม่ๆ เพื่อนำมาต่อสู้กับปัญหาเชื้อมาลาเรียดื้อยา อย่างไรก็ตามความคืบหน้าของการพัฒนายาต้านมาลาเรียยังมีข้อจำกัดอันเนื่องมาจากการขาดแคลนเครื่องมือทางรีเวอร์สเจเนติกส์สำหรับการพิสูจน์เป้าหมายของยาใหม่ๆ และการศึกษากลไกการออกฤทธิ์ของยาใหม่ๆ โครงการวิจัยนี้มีวัตถุประสงค์ในการนำกลิมเอสไรโบไซม์ซึ่งเป็นเครื่องมือทางรีเวอร์สเจเนติกส์ที่ได้ถูกพัฒนาขึ้นในห้องปฏิบัติการฯ ของคณะผู้วิจัยมาใช้ในการศึกษายีนที่สำคัญรวมไปถึงการพิสูจน์ยีนที่อาจเป็นเป้าหมายของยาต้านมาลาเรียในเชื้อพลาสโมเดียมฟาลซิปารัมซึ่งเป็นเชื้อที่ก่อให้เกิดโรคมาลาเรียในคน กลิมเอสไรโบไซม์สามารถถูกกระตุ้นด้วยน้ำตาลกลูโคซามีนให้ตัดสายลำดับเบสเอ็มอาร์เอ็นเอของตัวเองออก จึงมีการนำกลิมเอสไรโบไซม์มาใช้ในการควบคุมการแสดงออกของยีนในเชื้อมาลาเรีย ในโครงการวิจัยนี้คณะผู้วิจัยได้สร้างเชื้อมาลาเรียปรับแต่งพันธุกรรมที่ถูกแทรกลำดับเบสของกลิมเอสไรโบไซม์เข้าไปที่ท้ายของยีนไดไฮโดรโฟเลทรีดักเทสไธมิดิเลทซินเทส (DHFR-TS) และยีนดีอ๊อกซีไฮพิวซีนซินเธส (DHS) ในสภาวะที่มีน้ำตาลกลูโคซามีนพบว่าเชื้อปรับแต่งพันธุกรรมมีการลดการแสดงออกของยีนดังกล่าวได้ถึงสิบเท่าเมื่อเปรียบเทียบกับในสภาวะปกติ ทั้งนี้ได้มีการสร้างเชื้อมาลาเรียปรับแต่งพันธุกรรมที่ถูกแทรกลำดับเบสของกลิมเอสไรโบไซม์ชนิดกลายพันธุ์ซึ่งจะไม่ถูกกระตุ้นด้วยน้ำตาลกลูโคซามีนเข้าไปที่ท้ายของยีน DHS อีกด้วย ในกรณีนี้ไม่พบการลดการแสดงออกของยีน DHS ในเชื้อปรับแต่งพันธุกรรมแม้ว่าจะมีการเติมน้ำตาลกลูโคซามีน การลดการแสดงออกของยีน DHFR-TS หรือ DHS ในเชื้อปรับแต่งพันธุกรรม ส่งผลให้เชื้อมีการเจริญเติบโตที่ลดลงอย่างมีนัยสำคัญ เป็นการพิสูจน์ว่ายีนทั้งสองนี้เป็นยีนที่สำคัญในเชื้อพลาสโมเดียมฟาลซิปารัม นอกจากนี้คณะผู้วิจัยได้พัฒนาวิธีที่เรียกว่า Chemogenomic profiling เพื่อพิสูจน์ยีนที่เป็นเป้าหมายของสารออกฤทธิ์ต้านมาลาเรีย โดยการตรวจสอบความไวของเชื้อปรับแต่งพันธุกรรมต่อสารออกฤทธิ์ต้านมาลาเรียในสภาวะที่ถูกลดการแสดงออกของยีนเปรียบเทียบกับสภาวะปกติ จากผลการทดลองพบว่าเชื้อที่ถูกลดการแสดงออกของยีนที่เป็นเป้าหมายของยาหรือสารออกฤทธิ์ต้านมาลาเรียจะมีความไวต่อยาหรือสารนั้นๆสูงขึ้นเมื่อเปรียบเทียบกับเชื้อที่มีการแสดงออกของยีนปกติ จากหลักการดังกล่าวคณะผู้วิจัยได้นำเชื้อปรับแต่งพันธุกรรมที่มีลำดับเบสของกลิมเอสไรโบไซม์แทรกที่ท้ายของยีน DHFR-TS มาทดสอบกับสารออกฤทธิ์ต้านมาลาเรีย 400 สารจากคลังสารมาลาเรียบ๊อกซ์ ทำให้สามารถพิสูจน์กลไกการออกฤทธิ์ของสารออกฤทธิ์ต้านมาลาเรียได้ 2 สารที่มุ่งเป้าต่อยีน DHFR-TS และจากวิธี Chemogenomic profiling นี้สามารถพิสูจน์ได้ว่ายีน DHS ในเชื้อพลาสโมเดียมฟาลซิปารัมเป็นเป้าหมายของสาร N1-guanyl-1, 7-diaminoheptane ซึ่งเป็นสารยับยั้งการทำงานของโปรตีน DHS ในสิ่งมีชีวิตอื่นๆ อีกด้วย โดยสรุป โครงการวิจัยนี้สามารถพิสูจน์ว่ายีน DHS เป็นเป้าหมายของยาต้านมาลาเรียใหม่ได้ และยังสามารถพิสูจน์กลไกการออกฤทธิ์ของสารออกฤทธิ์ต้านมาลาเรียใหม่ได้อีก 2 สารอีกด้วย คณะผู้วิจัยมีความคาดหวังว่าการใช้กลิมเอสไรโบไซม์ซึ่งเป็นเครื่องมือทางรีเวอร์สเจเนติกส์และการใช้วิธี Chemogenomic profiling จะสามารถนำไปสู่การพิสูจน์เป้าหมายของยาต้านมาลาเรียใหม่ๆ รวมไปถึงการค้นพบกลไกการออกฤทธิ์ของยาหรือสารใหม่ๆ เพิ่มขึ้นได้ในอนาคต

Executive Summary

Overview and project aim

The aim of the project was to create transgenic *Plasmodium falciparum* malaria parasites carrying modifications of putative essential genes. The transgenic DNA included the *glmS* ribozyme, which is a reverse-genetic tool for attenuating gene expression. If the targeted gene is essential, attenuation of expression leads to inhibition of parasite growth and increased sensitivity to antimalarials acting on the gene product.

Methods

Gene targeting sequences were PCR amplified and cloned into plasmids. The plasmid vectors contained green fluorescent protein (GFP) and *glmS* ribozyme sequences for monitoring target protein and attenuation of expression, respectively. For each gene target, plasmid vectors with wild-type *glmS* and inactive M9 variant ribozyme were constructed. The plasmids were transfected into *P. falciparum* parasites. Transgenic parasites with integration of plasmid DNA were selected by drug cycling, and clones isolated by limiting dilution. Integrants were detected by PCR assay and fluorescence microscopy. Attenuation of target gene expression was assessed by flow cytometry and western blotting. The growth of transgenic parasites under conditions of target gene attenuation were assessed by co-culture with a control transgenic parasite. Test:control parasite ratios were measured by quantitative PCR. Chemogenomic profiling was performed by culturing parasites with varying concentrations of antimalarial compounds under normal and gene-attenuated conditions. The data were fitted to dose-response models, and inhibition constants were reported. Compounds targeting the gene of interest were identified as those which showed significantly greater inhibition constant in the normal condition compared with gene-attenuated condition using F-statistical tests.

Findings

13 genes were identified as putatively essential and novel drug targets from literature search of *in silico* prediction studies (section 4.1). 24 plasmids were constructed for transfection of *Plasmodium falciparum* malaria parasites, in which modifications of 10 genes were attempted (section 4.2). Integration was detected at the dihydrofolate reductase-thymidylate synthase (DHFR-TS), deoxyhypusine synthase (DHS), thioredoxin reductase (TRXR), adenosine deaminase (ADA) and chorismate synthase (CS) genes. Clonal integrant transgenic parasites were obtained for DHS and DHFR-TS. The DHS integrants included lines with wild-type and M9 variant ribozymes. The DHFR-TS integrant was established in the K1 strain and carried the active *glmS* ribozyme. Attenuation of target gene expression in transgenic integrant parasites was demonstrated by treatment with D-glucosamine (GlcN), the cofactor required for ribozyme

activity (section 4.3). The concentration of GlcN needed for 50% reduction of DHFR-TS target protein expression ($EC_{50)}$ is approximately 0.4 mM in the K1 background, compared with 0.8 mM in the 3D7 background. The DHS protein under control of wild-type *glmS* ribozyme is attenuated with approximately the same efficiency. No attenuation of DHS protein was observed in the transgenic parasite carrying the M9 variant ribozyme. Attenuation of DHFR-TS and DHS protein expression in transgenic parasites led to a significant growth defect, validating these genes as essential (section 4.4). Chemogenomic profiling (section 4.5) showed that antifolate drugs (pyrimethamine, cycloguanil, methotrexate, WR99210) and the experimental compounds MMV667486 and MMV667487 target DHFR-TS, whereas N1-guanyl-1,7-diaminoheptane targets DHS. Refinement of the *glmS* ribozyme tool efficiency was attempted by measuring gene expression levels with the ribozyme in different positions relative to the target gene (section 4.6). When located in the 5′ UTR, the ribozyme strongly inhibits target gene expression even in the absence of GlcN.

Conclusions

-Novel antimalarial targets, such as the DHS gene, can be identified using the *glmS* ribozyme tool

-Chemogenomic profiling using the *glmS* ribozyme tool can identify antimalarial mode of action

Recommendations

-Integration of transfection DNA is difficult for some gene targets. Genome editing tools such as CRISPR-Cas9 could be useful in these cases.

-The *glmS* ribozyme needs to be inserted in the 3′ UTR position relative to the target gene for controlling gene expression conditional on GlcN treatment.

Limitations

The difficulty in integrating transfection DNA limited testing of gene essentiality to only 1 of 13 novel candidate genes selected for study. The expression of target genes with *glmS* ribozyme integration can be attenuated up to ten fold, which may be insufficient to observe a loss of function phenotype, depending on the phenotypic assay used. This limitation could prevent conclusions being drawn about gene function, especially if the gene is robust, i.e. only a very low level of normal gene activity is necessary for viability.

Table of Contents

1. Background

Malaria is major infectious disease in which millions of people worldwide succumb to every year. Although the incidence of malaria is declining owing to efforts to control the disease, such as improving access to antimalarial drugs, there is concern that malaria may undergo resurgence (Tanner et al., 2015). This fear is based on the emergence and spread of drug-resistant malaria parasites. Artemisinin-resistant *Plasmodium falciparum* malaria parasites in Southeast Asia are starting to evolve cross-resistance to partner drugs, which could render the World Health Organization-recommended artemisinin combination therapies (ACT) ineffective in the near future (Imwong et al., 2017). Current alternative drugs are not as effective as ACT, and so research into new antimalarials is urgently needed to avert a potential public health crisis.

When cross-resistance to different drugs is established in the malaria parasite population, development of new drugs is more challenging because fewer active compounds are likely to be found from empirical screening of compound libraries. This is because resistant parasites are also resistant to structurally related compounds that have similar modes of action. In this situation, rational design of inhibitors against a specific target molecule (target-based drug development) is more likely to yield compounds with the required anti-malarial activity against drug-resistant parasites, as shown by the development of the P218 compound targeting pyrimethamine-resistant *P. falciparum* DHFR-TS (Yuthavong et al., 2012). The major obstacles to the target-based approach for development of new antimalarials are that very few drug targets are known, and the mode of action of many compounds with anti-malarial activity is also unknown. For a gene product to be an antimalarial target, it must be essential. If the putative drug target is an enzyme, it must be part of an essential non-redundant pathway. Screening for inhibitory compounds is expensive and requires much effort; hence, target validation is a necessary precondition before embarking on these endeavors. There are potentially many gene targets yet to be explored, since the majority of the *P. falciparum* genes have unknown functions.

A good proof of target validation is gene knockout in which DNA fragments matching the gene target of interest are introduced into the parasite cell via a plasmid DNA construct. The target gene is ablated by homologous recombination, and genetically modified parasites carrying the knocked-out gene can be selected for and characterized (Waterkeyn et al., 1999); (de Koning-Ward et al., 2015). A stumbling block to this approach is that the parasite is haploid throughout most of its life-cycle, including the asexual stages which can be cultured in the laboratory. Therefore, parasite genes important for growth cannot be knocked-out, since parasites carrying such disrupted genes would stop growing and die before they can be isolated and studied in the laboratory. Currently, the only proof currently available to researchers that a gene target is

essential is by making repeated attempts at gene knockout. If knockout is unsuccessful, the target is said to be validated. Clearly, this is insufficient proof as there is no direct evidence of the target's essentiality and no mutant phenotype can be observed to understand the gene's function. When gene knockout is not available, RNA interference (RNAi) is a commonly used method to attenuate gene expression in model organisms. Unfortunately, this tool is ineffective in *Plasmodium* parasites as they lack the RNAi machinery (Baum et al., 2009). Alternative genetic tools, such as the destabilizing domain (DD) tools (Armstrong and Goldberg, 2007); (Muralidharan et al., 2011) have been developed for conditional regulation of *P. falciparum* gene expression. The DD tools work by transgenic modification of the target gene, such that the encoded protein is expressed as a fusion protein to the DD. The level of the target protein is controlled by adding a stabilizer ligand, which stabilizes the folding of the DD. Although several essential parasite genes have been identified with these tools, they are not generally applicable. In several cases, it has been found that the DD can interfere with the normal function of the parasite protein it is fused to, or the efficiency of attenuation is too low to be useful (Shaw and Aroonsri, 2017).

The limitation of inadequate genetic tools has severely hampered malaria research, especially the development of drugs and vaccines to control the disease. The mechanism of how most antimalarials work is poorly understood, since parasites carrying disruptions of genes essential for growth, which includes the targets of drugs, are not available. A portfolio of diverse drugs against several different targets is urgently needed to eliminate parasites resistant to existing antimalarials. To obtain this portfolio, we need to identify new targets and understand the mechanism of action of antimalarials using genetic tools. We developed the *glmS* ribozyme genetic tool for filling this need in malaria research, in particular drug development. The *glmS* ribozyme is a gene regulatory element found upstream of the glucosamine-6-phosphate synthetase (*glmS*) gene in many species of bacteria (McCown et al., 2011). The *glmS* ribozyme is a catalytic self-cleaving RNA which requires the cofactor glucosamine-6-phosphate (GlcN6P) for activation (Winkler et al., 2004). We hypothesized that a sequence encoding the natural *glmS* ribozyme regulatory element from *Bacillus subtilis* bacteria (Winkler et al., 2004) could be inserted into a gene of interest using conventional DNA transfection techniques. The *glmS* element is inserted downstream of the gene target so that when the gene is transcribed, a chimeric mRNA is produced. Under normal growth conditions, GlcN6P is limiting and the mRNA can be translated to protein. The *glmS* ribozyme can be activated by supplementing the in vitro parasite culture medium with exogenous glucosamine (GlcN). Upon activation of the *glmS* ribozyme, the mRNA is separated from its 3′ polyA tail and then degraded by the parasite's RNA exosome machinery, resulting in reduction of translation and protein product. A schematic of how the tool works is shown in Figure 1. .

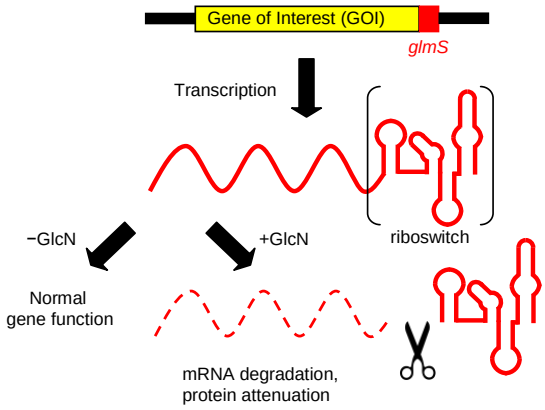

Figure 1. Schematic of the *glmS* ribozyme reverse-genetic tool.

The *glmS* ribozyme element is inserted by DNA transfection downstream of the gene of interest (GOI). A chimeric mRNA is transcribed from the modified gene, in which the *glmS* ribozyme adopts its ribozyme catalytic conformation (indicated by the braces). Under normal growth conditions, the ribozyme-activating ligand is limiting and the gene functions normally. Upon treatment of transgenic parasites with glucosamine (GlcN), self-cleavage of the ribozyme is activated and the body of the gene mRNA is separated from the polyA at the 3′ end. Cleaved mRNA is degraded by the parasite's RNA exosome machinery, leading to reduction of translation and gene expression (Figure published in (Shaw and Aroonsri, 2017)).

We demonstrated proof of concept that the *glmS* ribozyme tool can function in *Plasmodium falciparum* (Prommana et al., 2013). In this work, it was shown that the expression of a reporter gene bearing a *glmS* ribozyme can be reduced up to 10-fold by adding GlcN to the parasite culture medium. The efficiency of the *glmS* ribozyme tool is thus greater than the previously described DD tools. Furthermore, we showed that an endogenous essential gene can be controlled using the *glmS* ribozyme in which the *P. falciparum* dihydrofolate reductase-thymidylate synthase (DHFR-TS) gene was modified by inserting the *glmS* ribozyme element. The DHFR-TS gene encodes a bifunctional enzyme which is known to have an essential function in the folate and de novo pyrimidine synthesis pathways. Moreover, DHFR-TS is the known target of antifolate antimalarial drugs such as pyrimethamine (Yuvaniyama et al., 2003). Treatment of transgenic parasites with GlcN led to specific attenuation of DHFR-TS expression and growth arrest (Prommana et al., 2013). Furthermore, attenuation of DHFR-TS expression sensitizes transgenic parasites to pyrimethamine (Prommana et al., 2013). From these data, we proposed that the *glmS* ribozyme tool can be used to identify new antimalarial targets and determine mode of action of antimalarial compounds.

2. Objectives

The main objective of the project was to establish transgenic parasite lines with the *glmS* ribozyme element integrated at several candidate drug target genes. The transgenic parasites are employed in phenotypic assays to study target gene function. The first goal was to demonstrate that target gene expression can be attenuated in transgenic parasites by GlcN treatment, which is hypothesized to activate the *glmS* ribozyme *in vivo*. The second goal was to perform growth assays in transgenic parasites, testing the effect of GlcN treatment on growth. If a GlcN-dependent growth defect is observed, the target is validated as an essential gene and drug target. The third goal was to establish a chemogenomic profiling method for determining mode of action of antimalarials using the transgenic parasites. The fourth goal was to refine the *glmS* ribozyme tool to make it more efficient for attenuating target gene expression.

3. Methodology

3.1 In silico identification of putative essential genes

Candidate essential gene targets were identified by a meta-analysis of published articles describing essential genes in *P. falciparum* predicted using different bioinformatic approaches (Yeh et al., 2004); (Fatumo et al., 2009); (Crowther et al., 2010); (Huthmacher et al., 2010); (Plata et al., 2010); (Fatumo et al., 2011); (Ludin et al., 2012); (Yadav et al., 2013). Lists of predicted essential genes were prepared from each study, and the union of all eight showed 176 genes in total. A consensus voting scheme was employed for meta-analysis, in which genes predicted as essential in more than one study were accorded as candidates for this study.

3.2 Cloning and construction of transfection plasmids

Two destination plasmids for cloning of homologous targeting sequences were constructed from the published plasmids from published plasmids pGFP_*glmS* and pGFP_M9 (Prommana et al., 2013), in which the unnecessary hsp86 promoter and REP20 sequences were removed by digestion with *Afl*II and *Bgl*II. The remaining 6.7 kb vector fragment were end-repaired by T4 DNA polymerase treatment and self-religated using T4 DNA ligase, resulting in plasmids simplified-pGFP_glmS and simplified-pGFP_M9, respectively, which have the blasticidin S deaminase gene (BSD) as a transgenic parasite selectable marker. Both plasmids were digested with *Nhe*I and *Kpn*I (New England Biolabs, USA) to receive gene targeting fragments at the correct position with respect to green fluorescent protein (GFP) protein marker and *glmS* ribozyme sequence (Figure 2).

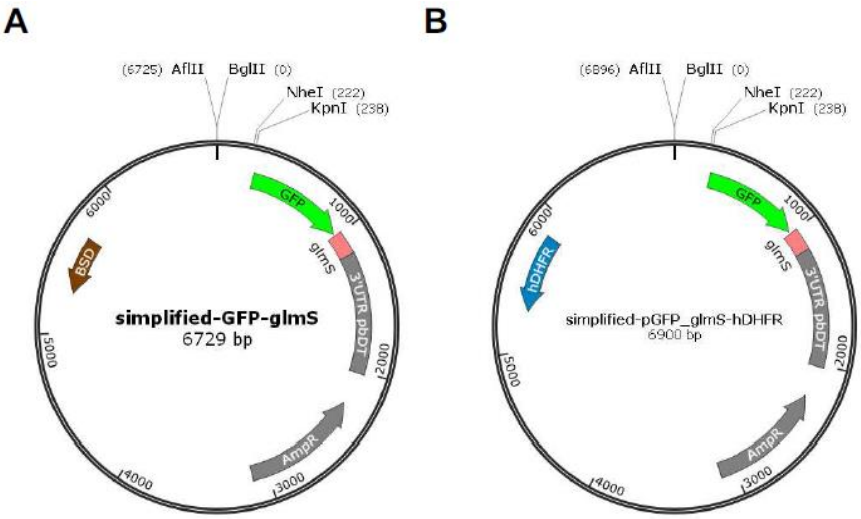

Figure 2. Plasmid maps of simplified-pGFP-glmS (A) and simplified-pGFP-glmS-hDHFR (B) vectors constructed for *P. falciparum* transfection.

Relevant functional sequences are indicated by the colored bars/arrows. Specific gene targeting sequence was cloned into the vectors via the *Nhe*I and *Kpn*I sites. The targeting sequence is in-frame with green fluorescent protein (GFP) coding sequence to facilitate monitoring of protein levels and sub-cellular localization in transgenic parasites. The *glmS* ribozyme sequence is located immediately downstream of the open reading frame. The M9 versions of these vectors contain ribozyme-inactivating mutations in the *glmS* sequence; these plasmids are used as controls in knockdown experiments to control for confounding toxicity of the GlcN inducer. The genes blasticidin S deaminase (BSD) and human dihydrofolate reductase (hDHFR) are used for transgenic selection with blasticidin S and WR99210, respectively.

Gene fragments from selected candidate essential genes were obtained by PCR amplification from *P. falciparum* strain 3D7 (reference strain) genomic DNA. Parasite genomic DNA was obtained using a blood genomic DNA kit (Qiagen, Germany) following the manufacturer's recommendations. PCR primers were synthesized as oligonucleotides with standard desalting from the IDT (Singapore) or Macrogen (Korea) companies. PCR was conducted for each gene targeting primer pair in separate reactions using 1-100 ng of parasite genomic DNA template. PCR was performed using the Phusion enzyme following the manufacturer's recommendations (New England Biolabs, USA). PCR primers were designed from gene sequences annotated in PlasmoDB (Aurrecoechea et al., 2009). Forward and reverse primers were designed to amplify 3′ end gene fragments 300-1000 bp in length. The PCR primers also include 18-20 nucleotide sequences at the 5′ end that overlap with the terminal sequences of *Nhe*I-*Kpn*I digested plasmid vectors. The vector overlap sequence was designed for cloning using the Gibson assembly method

(Gibson et al., 2009). All reverse primers contain a substitution changing the stop codon to a Ser (Table 1), of each target gene for resulting gene product with green fluorescence protein (GFP) epitope tag at C-termini. PCR products of homology targeting sequences were cloned into plasmids using the Gibson assembly master mix (New England Biolabs). Assembled DNA reactions were transformed into *Escherichia coli* XL-10 Gold (Stratagene, USA). Plasmids were extracted and purified from recombinant transformed cells by the alkaline lysis method (Feliciello and Chinali, 1993). All plasmids were verified by restriction mapping and BigDye capillary Sanger DNA sequencing (1st BASE, Malaysia). Large-scale preparations of each plasmid from 100-200 mL of bacterial culture were performed to obtain sufficient plasmid DNA for *P. falciparum* 3D7 transfection by the alkaline lysis method (Feliciello and Chinali, 1993).

Plasmid name	*Gene symbol*	*Forward primer 5′—3′*	*Reverse primer 5′—3′*
Sim-pGFP-glmS-ADA	ADA	*AAATGTTATCAGACCTAGCG*ATGAGTGATGAAGAAATTAT	*TTGTTGCTCTTGAGGTACC*TGAAAAATATTTACTTATAATTTTATT
Sim-pGFP-M9-ADA	ADA		
Sim-pGFP-glmS-CS	CS	*AAATGTTATCAGACCTAGCG*TTAGTAGATTCTTATGGAAC	*TTGTTGCTCTTGAGGTACC*TGACATATTCCTAAACAAT
Sim-pGFP-M9-CS	CS		
Sim-pGFP-glmS-DHODH	DHODH	*AAATGTTATCAGACCTAGCG*TTATCGAAATTGGTACCATA	*TTGTTGCTCTTGAGGTACC*TGAACTTTTGCTATGCTTTC
Sim-pGFP-M9-DHODH	DHODH		
Sim-pGFP-glmS-DHS	DHS	*AAATGTTATCAGACCTAGCG*ATCACGTTTCTTTTAAAGAG	*TTGTTGCTCTTGAGGTACC*TGACATATCTTTTTTCCTCT
Sim-pGFP-M9-DHS	DHS		
Sim-pGFP-glmS-FBA	FBA	*AAATGTTATCAGACCTAGCG*AATTAGAGAACACAATAGAA	*TTGTTGCTCTTGAGGTACC*TGAATAGACATATTTCTTTTCA
Sim-pGFP-M9-FBA	FBA		
Sim-pGFP-glmS-GPAT	GPAT	*AAATGTTATCAGACCTAGCG*ATGCCAGATTTTTACTTTT	*TTGTTGCTCTTGAGGTACC*TGATAATATCTCTTCTTTGTATTC
Sim-pGFP-M9-GPAT	GPAT		
Sim-pGFP-glmS-OPRT	OPRT	*AAATGTTATCAGACCTAGCG*ATAAGATATGTGAGGAAAGA	*TTGTTGCTCTTGAGGTACC*TGATATCATCGACTGTATATC
Sim-pGFP-M9-OPRT	OPRT		
Sim-pGFP-glmS-SAHH	SAHH	*AAATGTTATCAGACCTAGCG*ATGGTTGAAAATAAGAGTAAG	*TTGTTGCTCTTGAGGTACC*TGAATATCTGTATTCGTTACT
Sim-pGFP-M9-SAHH	SAHH		
Sim-pGFP-glmS-RNR	RNR	*AAATGTTATCAGACCTAGCG*ATGGCTGATGTTATAAACAT	*TTGTTGCTCTTGAGGTACC*TGAAAATTCCGTATTCAGA
Sim-pGFP-M9-RNR	RNR		
Sim-pGFP-glmS-TRXR	TRXR	*AAATGTTATCAGACCTAGCG*AGACCACATATACCAGAT	*TTGTTGCTCTTGAGGTACC*TGATCCACATTTTCCAC
Sim-pGFP-M9-TRXR	TRXR		

Sim-pGFP-glmS-CS-hDHFR	CS	NA	NA
Sim-pGFP-glmS-DHODH-hDHFR	DHODH	NA	NA
Sim-pGFP-glmS-OPRT-hDHFR	OPRT	NA	NA
Sim-pGFP-glmS-TRXR-hDHFR	TRXR	NA	NA

Table 1. List of plasmids constructed for transgenic modification of *Plasmodium falciparum* candidate essential genes.

For each candidate gene (indicated by the gene symbol), targeting sequences for homologous recombination were obtained by PCR using forward and reverse primer pairs indicated in the third and fourth columns, respectively. Sequences overlapping the plasmid vector used for cloning by Gibson assembly are italicized. The nucleotides substituting the stop codon to a Ser codon in reverse primers are underlined. For plasmids with cells labeled NA, The targeting sequences for homologous recombination were subcloned from the equivalent plasmid with the blasticidin S deaminase selectable marker gene, e.g. the CS gene targeting sequence in plasmid Sim-pGFP-glmS-CS-hDHFR was subcloned from plasmid Sim-pGFP-glmS-CS.

Four plasmids for study of episomally-expressed reporter genes were constructed for transfection experiments. The pGFP_*glmS* plasmid (Prommana et al., 2013) was modified to create transfection plasmids pHAEGFP_hDHFR, p5Rbz_HAEGFP_hDHFR, p3Rbz_HAEGFP_hDHFR and p53Rbz_HAEGFP_hDHFR. All these plasmids contain a reporter gene coding for a HAEGFP-hDHFR fusion protein. The fusion protein thus has three protein moieties. The hemagglutinin (HA) tag is an epitope tag suitable for detection by western blot with commercial anti-HA antibodies (Schembri et al., 2007). The enhanced green fluorescent protein (EGFP) moiety allows enumeration of transgenic parasites by flow cytometry and fluorescence microscopy (Cormack et al., 1996). The human dihydrofolate reductase (hDHFR) moiety confers parasite resistance to antifolate compounds, including WR99210 (Fidock and Wellems, 1997). The reporter gene is flanked by *P. falciparum* promoter and terminator elements, which drive strong expression during the blood stages of parasite development (Prommana et al., 2013). The pHAEGFP_hDHFR plasmid contains no ribozyme element and thus serves as a control. The reporter gene from this plasmid is expected to show strong activity in transfected parasites, and its expression should not be affected by GlcN treatment. The HAEGFP gene was PCR amplified from plasmid pcDNA5-FRT-kozak-HA-EGFP-Halotag2 ((Neklesa et al., 2011); a gift from Taavi Neklesa, Yale Uni, USA) using primers: 5′-GGAGGAAGAAAAATATGGCATACCCTTAT GACGTACCTGACTA-3′ and 5′-CGGGGTACCGCTACCTCCGCCACCACTTCCACCGCCT CCAGAACCTCCTCCACCCTTGTACAGCTCGTCCATG-3′. The 5′-*glmS* ribozyme was PCR amplified from a plasmid containing the cloned *B. subtilis glmS* ribozyme sequence (Winkler et al., 2004) using primers: 5′- CGCGGATCCTATAATTATAGCGCCCGAACTAA-3′ and 5′-CCTCCTACATGTTTTTTGGAAGATCATGTGATTTCTCTTTGTTC-3′. The 5′ *glmS* ribozyme also included the entire native 5′ UTR sequence of the *B. subtilis glmS* gene (Winkler et al., 2004) to minimize potential translational interference caused by ribozyme secondary structure. A linker sequence to join the *glmS* ribozyme sequence with the HAEGFP gene was obtained by gene synthesis PCR of overlapping oligonucleotides: 5′-TCCAAAAAACATGTAGGAGGGG ACGATTGAAAGTCCCCTTGAAATTTGACTTTCTTCG-3′ and 5′-TGCCATATTTTTCTT CCTCCTAAGATTGTAAAAGGAGACGAAGAAAGTCAAATTTCAAGG-3. The HAEGFP, 5′-*glmS* ribozyme and linker sequence amplicons were combined and used as templates for gene synthesis PCR using primers: 5′- CGCGGATCCTATAATTATAGCGCCCGAACTAA-3′ and 5′-CGGGGTACCGCTACCTCCGCCACCACTTCCACCGCCTCCAGAACCTCCTCCACCCTTG TACAGCTCGTCCATG-3′. The 1070 bp amplicon from gene synthesis was digested with *Bam*HI and *Kpn*I, and cloned into *Bam*HI-*Kpn*I digested plasmid pRSETc (Invitrogen, USA) to create plasmid pRSETc_HAEGFP*glmS*. The hDHFR gene was PCR-amplified from plasmid pL0035 (Braks et al., 2006) using primers: 5′-CGGGGTACCATGGTTGGTTCGCTAAACTG-3′ and 5′-AAAACTGCAGTTAATCATTCTTCTCATATACTTCAAATTTG-3′. The hDHFR

amplicon was digested with *Kpn*I and ligated to *Kpn*I-digested pRSETc_HAEGFP*glmS*. The ligation product was used as a template for PCR using primers: 5′-CGCGGATCCAAAAATA TGGCATACCCTTATGA-3′ and 5′-ACCGCTCGAGTTAATCATTCTTCTCATATACTTCA AATTTG-3′ (noRbz amplicon); 5′-CGCGGATCCAAAAATATGGCATACCCTTATGA-3′ and 5′-AAAACTGCAGTTAATCATTCTTCTCATATACTTCAAATTTG-3′ (3Rbz amplicon); 5′- CGCGGATCCTATAATTATAGCGCCCGAACTAA-3′ and 5′-ACCGCTCGAGTTAAT CATTCTTCTCATATACTTCAAATTTG-3′ (5Rbz amplicon); 5′- CGCGGATCCTATAATTA TAGCGCCCGAACTAA-3′ and 5′-AAAACTGCAGTTAATCATTCTTCTCATATACTTCAA ATTTG-3′ (53Rbz amplicon). The noRBZ and 5Rbz amplicons were digested with *Bgl*II and *Pst*I. The 3Rbz and 53Rbz amplicons were digested with *Bgl*II and *Xho*I. Digested amplicons were sub-cloned into plasmid pGFP_*glmS* (Prommana et al., 2013) digested with the appropriate restriction enzymes. The sequences of all plasmids were validated by BigDye capillary Sanger sequencing (Macrogen, Korea).

3.3 Parasite culture and DNA transfection

P. falciparum strain 3D7 (reference strain) was cultured *in vitro* following the standard method (Trager and Jensen, 1976), with the modification of 0.5% Albumax I (Gibco® Life Technologies, USA) replacing human serum (Cranmer et al., 1997). Human O+ erythrocytes were obtained from donors. Human erythrocytes were obtained from donors after providing informed consent, following a protocol approved by the National Science and Technology Development Agency (NSTDA), Pathum Thani, Thailand, Ethics Committee for Human Research, document no. 0006/2557. 2% haematocrit was used for most parasite cultures, with slightly higher haematocrit (up to 4%) used during drug selection steps of DNA transfection. Parasites were synchronized to ring stages using the sorbitol treatment method (Lambros and Vanderberg, 1979). 50-100 μg of plasmid DNA were used for each parasite transfection experiment. DNA was transfected either using the method of direct electroporation of ring-stage infected erythrocytes (Wu et al., 1995), or by the method of preloading erythrocytes with DNA prior to parasite invasion (Deitsch et al., 2001). Treatments of parasites with 2 μg/ml blasticidin S or 2 nM WR99210 were performed to select transgenic parasites carrying BSD and hDHFR selective marker, respectively. Drug was added to parasite culture 48 hours post-electroporation, and parasites were cultured under drug selection until resistant parasites emerged (typically 3 weeks). To obtain parasites with chromosomal integration of the plasmid, parasites were cultured in the absence of drug for 3 weeks. During this period, episomes are lost in replicating parasites as they have no mechanism for segregating episomes. The drug on-off cycle (3 weeks each) was repeated to enrich for integrant parasites in the population. Integrants were detected by PCR assay using

integration-specific primers, in which PCR products are detected only when integration at the desired locus has occurred (Figure 3).

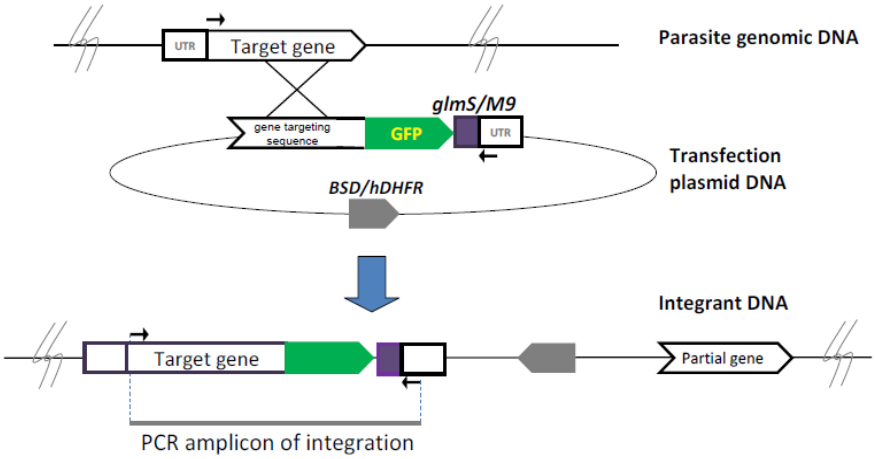

Figure 3. Schematic of gene targeting integration strategy for *P. falciparum* employed in this study.

P. falciparum parasites are transfected with plasmid DNA containing gene targeting sequence, the green fluorescent protein (GFP) gene, the *glmS* ribozyme element (wild-type *glmS* or inactive M9 variant) and a transgenic selectable marker gene (blasticidin S deaminase (BSD), or human dihydrofolate reductase (hDHFR)). After integration by single cross-over recombination, the GFP is integrated in-frame with the gene of interest, so that a fusion protein is produced from the modified gene and the ribozyme is expressed as RNA in the 3′ untranslated region (UTR) position. Small arrows indicate oligonucleotide primers for PCR assay of integration, which yield product (PCR amplicon of integration) only from cells which have undergone single cross-over homologous recombination at the target gene.

3.4 Co-culture growth inhibition assays

P. falciparum transgenic parasite line *Pf*FC_*glmS* was provided by Ms. Navaporn Posayapisit (unpublished data, Posayapisit, Uthaipibull and Kamchonwongpaisan, pers. comm.). This parasite line has the *glmS* ribozyme element integrated at the ferrochelatase (FC) encoding gene, PF3D7_1364900. This parasite line was established by DNA transfection as outlined in section 3.3. Integration of the *glmS* ribozyme element at the ferrochelatase (FC) encoding gene, PF3D7_1364900 was confirmed by integration-specific PCR and Southern blot experiments (unpublished data, Ms. Navaporn Posayapisit pers. comm.). The growth of a test transgenic line with *glmS* ribozyme element integrated at a putative essential gene was normalized to that of the *Pf*FC_*glmS* control. In this manner, extended growth assays can be conducted with the confounding effects of the inducer and transgenic selective agent accounted for. The control and test transgenic lines were first cultured separately and synchronized as described in section 3.3. The ring-stage synchronized parasites were diluted to approximately 0.5% parasitemia. A new culture was established by combining control and test transgenic parasite cultures (5 mL of each)

into the same culture plate. Samples were taken from the parasite co-culture every 4 days for 21 days (10 growth cycles). At each time-point, the culture reached a parasitemia of approximately 2.5%, consisting of mostly trophozoite stage parasites. The culture was then diluted to approximately 0.1% parasitemia in fresh medium and continued. The parasite culture plates were placed in a refrigerator on "ring" days for 5-7 hours to maintain high synchronization (Yuan et al., 2014). Parasite pellets were harvested from sub-culturing and used for genomic DNA extraction. The co-culture was conducted under standard and gene attenuation (2.5 or 5.0 mM GlcN inducer added) conditions, in which fresh GlcN was added after each time-point.

3.5 Quantitative PCR assay of transgenic parasite growth in co-culture experiments

Quantitative PCR (qPCR) assays were performed for measuring growth of transgenic parasites. Parasite genomic DNA was isolated from 1 mL culture samples using a blood genomic DNA kit (Qiagen, Germany) following the manufacturer's recommendations. Genomic DNA concentration was determined by Nanodrop and diluted to 10 ng / µL. Primers were designed to amplify specific discriminatory sequences in transgenic parasites. The discriminatory sequences spanned the fusion boundary between the 3′ end of the target gene and GFP. A primer pair was also designed to amplify the PF3D7_1324900 (L-lactate dehydrogenase) gene, which is present at single copy in all parasites and is used for normalization of template DNA input. qPCR experiments were performed using a CFX96 Touch^{TM} Real-Time PCR Detection System (Bio-Rad) and SsoFast EvaGreen Supermix (Bio-Rad) in 20 µL reaction volumes, as recommended by the manufacturer. For each qPCR reaction, 10 ng of gDNA and 500 nM of each forward and reverse primer were used. The following thermocycling conditions were used: 98^{o}C for 2 min; 40 cycles of 98^{o}C for 5 s and 60^{o}C for 5 s, followed by melt curve analysis from 65^{o}C to 95^{o}C with increments of 0.5^{o}C for 5 s. Primer pair efficiency was determined by serial dilution of genomic DNA templates. The TS-GFP amplicon was used to detect and quantify clonal transgenic parasite *Pf*DHFR-TS-*glmS* (Prommana et al., 2013), the DHS-GFP amplicon for *Pf*DHS_*glmS* and *Pf*DHS_M9 parasites, and the FC-GFP amplicon for *Pf*FC-*glmS* parasites. Quantification cycles (Cq) for each transgenic-integration specific amplicon (DHS-GFP, TS-GFP and FC-GFP) were transformed using the 2^{-Cq} function and normalized to LDH to give measurements of gene target abundance. The normalized abundance ratio of test target (DHS-GFP or TS-GFP) to control FC-GFP was taken as the value of growth relative to control. Growth data were analyzed using the lme4 package in R, which fits linear mixed effect models to the data (Bates et al., 2015). Linear models were constructed from the data using Maximum Likelihood and random slopes to account for variation among individual experiments. The null model was that growth varies as a function of time. The full model was that growth varies as a function of time with GlcN as a fixed effect. Significant differences in model fitting were assessed by likelihood ratio test, with $P<0.05$ considered significant.

3.6 Measurement of target gene expression in gene-attenuated transgenic parasites

The expression of modified target genes or episomally-maintained reporter genes in transgenic *P. falciparum* parasites was controlled using the *glmS* ribozyme, as described in (Prommana et al., 2013). Briefly, ring-stage synchronized parasites were treated with varying concentrations of GlcN (up to 10 mM) for 24 h and harvested. Target gene expression was measured by flow cytometry measuring the proportion of GFP-fluorescent cells, as described in (Prommana et al., 2013). The numbers of GFP-positive cells were normalized to the untreated sample, which was set as 100 %. Normalized GFP signal data were fitted to the four-parameter logistic dose response equation using the drc package in R (Ritz and Streibig, 2005). Target gene expression was also determined by Western blotting using anti-GFP polyclonal antibody, as described in (Prommana et al., 2013). Briefly, parasites were cultured in 60 mL at 4% haematocrit and synchronised to 8% ring-stages. The culture was divided equally into four plates and PBS (137 mM NaCl, 2.7 mM KCl, 8 mM Na_2HPO_4, 2 mM KH_2PO_4, pH 7.4) or GlcN added to obtain cultures with 0, 1.25, 2.5 or 5 mM GlcN, respectively. Parasites were harvested, released from host cells by saponin lysis and protein extracted by three cycles of freeze/thaw rupture. 18.5 µg of crude soluble protein extract was loaded into each lane of 12% SDS-PAGE gels. Equal loading was verified by Ponceau-S staining of the membrane after transfer. After GFP detection, the membrane was stripped and re-probed with anti-heat shock protein 70 (Hsp70) antibody (LifeSpan Biosciences, USA).

For the episomally-maintained reporter genes, the distribution of reporter gene expression in normal growth condition with no GlcN added was assessed by quantitative confocal microscopy measurement of GFP signal. The GFP intensities were assessed from 30- to 40- hour trophozoites. Specimens were analyzed on a model FV 1000D IX81 confocal laser scanning microscope (Olympus, Japan) controlled by software FV10-ASW 3.1 installed on the instrument. A 100X oil immersion objective lens (1.4 NA) was used. GFP was detected with an Argon laser 488 nm (500 nm excitation/600 nm emission; laser power 15%; high detector sensitivity 790 v; gain = 1 and offset = 7%). Images were obtained using a scan speed of 10.0 µs/pixel and were analyzed using FV10-ASW 3.0 Viewer software. The mean pixel density was determined in individual parasitized cells using the line tool. This value was taken as the GFP signal for that cell. The mean GFP signal from at least 49 cells in each group of transgenic parasite was compared with the non-fluorescent 3D7 reference strain parasite control using the Dunnett Contrasts method in the multcomp package in R (Herberich et al., 2010), in which $P<0.05$ was considered significant. The multcomp program applies simultaneous inference and robust covariance estimators for the multiple comparison procedure for assessing multiple means. In contrast to standard parametric ANOVA, no assumptions regarding the distribution, sample sizes or variance homogeneity are necessary, which reduces type I errors (Herberich et al., 2010).

3.7 Chemogenomic profiling of antimalarial compounds

Plasmodium falciparum ring-stage synchronized parasites were diluted with complete medium and human erythrocytes to 1% parasitemia and 2% haematocrit. Synchronized rings were maintained at 4 °C (Yuan et al., 2014) for up to 7 h before starting growth inhibition assays. Stock solutions of test compounds dissolved in DMSO were serially diluted in complete medium. Ten microlitres of each compound dilution were transferred into individual wells of 96-well microtitre plates. In addition to test compound, 10 μL of 1× PBS or 25 mM GlcN dissolved in 1x PBS were added into each well. 80 μL samples of ring-stage synchronized parasite, or uninfected erythrocyte suspension, were added last and the plates incubated in a gassed chamber at 37°C for 48 h. For experiments with known antimalarial drugs, parasite growth was measured by SYBR Green I staining and flow cytometry as described previously (Prommana et al., 2013). For screening of Malaria Box compounds (Spangenberg et al., 2013), three concentrations of each compound were tested. The concentrations tested varied according to the potency of the compound (50% effective concentration, EC_{50} reported by the Medicines for Malaria Venture (MMV)). EC_{50} estimates from the −GlcN control condition were necessary to correct for any systematic variation that could lead to substantial differences in EC_{50} compared with those reported by MMV. Moreover, we wished to develop a general screening method that could be applied to any compound library, including those not previously screened for antimalarial activity. Cells were lysed with 100 μL of SYBR Green I lysis buffer and fluorescence was measured with a Synergy Mx Monochromator-Based Multi-Mode Microplate Reader (BioTek, USA) with excitation and emission wavelength at 485 and 530 nm, respectively, and a gain setting equal to 50 to measure parasite DNA, as described previously (Smilkstein et al., 2004). The background fluorescence from the uninfected erythrocytes was subtracted to yield fluorescence measurements for analysis. The background corrected SYBR Green I signals from drug-treated parasites were normalized to the average background corrected signal from appropriate control parasites without drug (−GlcN measured separately from +GlcN) in the same experiment. Compound hits from screening were re-tested using the same culture conditions.

Growth data were normalized to appropriate −GlcN and +GlcN controls with no test compound added in the same experiment, which were taken as 100% growth. Dose–response growth inhibition assays were performed with seven to nine concentrations of test compounds. The data from dose-response assays of GlcN for attenuation of GFP expression were analyzed using the drc package in R (Ritz and Streibig, 2005) using the two parameter log-logistic regression model. To allow proper comparison of EC_{50} values between the −GlcN and +GlcN conditions, the maximum and minimum growth values were assigned as shared and constant between the two conditions, such that only two parameters (slope and EC_{50}) varied between the −GlcN and +GlcN conditions. EC_{50} ratios, associated S.Es and *F*-test statistics were calculated

from the two-variable parameter fitted models in the drc package. Log_2 EC_{50} ratios were considered significantly greater than zero at an *F*-test threshold of $P < 0.001$. Growth inhibition data from screening of MMV Malaria Box compounds were first pruned to remove low-potency compounds for which <50% inhibition of growth occurred under all concentrations tested. The two data points giving normalized growth inhibition lying either side of 50% inhibition were taken for estimating EC_{50} by simple linear interpolation, assuming a linear relationship of growth inhibition with log concentration of test compound.

4. Results

4.1 In silico identification of candidate essential genes

Literature review identified eight published bioinformatic studies from 2004 to 2013 of essential gene prediction for *P. falciparum*. Datasets of predicted essential genes were constructed from each study, which were cross-checked to ensure consistency of gene nomenclature and annotation. The union of all eight datasets showed 176 putative essential genes in total. A consensus voting scheme was employed for meta-analysis, in which genes predicted as essential in more than one dataset were accorded as candidates for this study. Among these 19 genes are two validated anti-malarial drug targets, bifunctional dihydrofolate reductase-thymidylate synthase (DHFR-TS) and dihydropteroate synthetase (DHPS). Since the purpose of the present study was to identify new targets, these genes were excluded for ribozyme targeting. Three genes, namely MAL1P2.40 (UMP-CMP kinase), MAL13P1.292 (Riboflavin kinase), PF14_0142 (Serine/threonine protein phosphatase) were also excluded since most chemical inhibitors of kinases and phosphatases are pleiotropic (multiple targets), and so our ribozyme targeting strategy is less likely to identify compounds with these genes as specific targets. The PFB0505c gene (Beta-ketoacyl-acyl carrier protein synthase III precursor) was excluded as it is known that the type II fatty acid synthesis pathway to which this gene belongs is non-essential in the blood stages (Vaughan et al., 2009). Finally, 13 genes were accorded high priority for ribozyme targeting, namely: ACT, ADA, CS, DHODH, DHS, FBA, GPAT, HPGRT, OPRT, PPAT, RNR, SAHH and TRXR (Table 2).

Table 2. *Plasmodium falciparum* candidate essential/drug target genes from literature search of bioinformatic prediction studies.

Gene ID	Annotation	Gene symbol	Pathway(s)	Studies gene identified as essential/drug target
PF14_0425	Fructose-bisphosphate aldolase	FBA	Glycolysis	(Yeh et al., 2004); (Crowther et al., 2010); (Fatumo et al., 2011); (Yadav et al., 2013)
PF10_0121	Hypoxanthine phosphoribosyltransferase	HGPRT	Purine salvage pathway	(Yeh et al., 2004); (Crowther et al., 2010); (Fatumo et al., 2011); (Yadav et al., 2013)
PFE0630c	Orotate phosphoribosyltransferase	OPRT	Pyrimidine metabolism	(Crowther et al., 2010); (Plata et al., 2010); (Yadav et al., 2013)
PF07_0018	Pantetheine-phosphate adenylyl transferase	PPAT	CoA biosynthesis	(Crowther et al., 2010); (Plata et al., 2010)
PF14_0125	Deoxyhypusine synthase	DHS	Activation of eIF5A (protein biosynthesis)	(Crowther et al., 2010); (Fatumo et al., 2009)
MAL13P1.221	Aspartate carbamoyltransferase	ACT	Pyrimidine metabolism	(Crowther et al., 2010); (Plata et al., 2010)
PF10_0289	Adenosine deaminase	ADA	Purine salvage pathway	(Crowther et al., 2010); (Fatumo et al., 2011)
PFE1050w	S-adenosyl-L-homocysteine hydrolase	SAHH	Cysteine/methionine metabolism	(Crowther et al., 2010); (Fatumo et al., 2011)
PFF1105c	Chorismate synthase	CS	Shikimate pathway	(Crowther et al., 2010); (Fatumo et al., 2011)
PFF0160c	Dihydroorotate dehydrogenase	DHODH	De novo pyrimidine biosynthesis, ETC	(Crowther et al., 2010); (Fatumo et al., 2011)
PF14_0053	Ribonucleotide reductase small subunit	RNR	Purine/pyrimidine metabolism	(Crowther et al., 2010); (Fatumo et al., 2011)
PFI1170c	Thioredoxin reductase	TRXR	Thioredoxin cycle, pyrimidine metabolism	(Crowther et al., 2010); (Fatumo et al., 2011)
PFL0620c	Glycerol-3-phosphate acyltransferase	GPAT	Phosphatidylethanolamine/phospatidylserine metabolism, choline transport	(Fatumo et al., 2011); (Ludin et al., 2012)

4.2. Creation of transgenic P. falciparum with modification of candidate essential genes

Partial gene targeting sequences for mediating integration of DNA at target gene loci were obtained by PCR from *P. falciparum* genomic DNA for all candidate genes except for ACT, HGPRT, and PPAT. PCR amplification of these gene sequences was unsuccessful despite testing a variety of PCR conditions (adjustment of primer annealing temperature, DNA polymerase, magnesium concentration, thermocycling parameters). Therefore, construction of transfection plasmids was performed for 10/13 candidate genes. Gene targeting sequences were cloned into *Nhe*I-*Kpn*I digested plasmid vectors. *P. falciparum* transfection experiments were performed with 24 plasmids (Table 1). After drug selection for transgenic parasites, integration was detected at four gene targets (ADA, CS, DHS, TRXR) by integration-specific PCR assay (Figure Figure 4.). Fluorescence microscopy analysis of these transgenic parasites revealed GFP-positive expressing cells for the CS, DHS, TRXR transfections, consistent with integration (the GFP is expressed as a fusion protein only after integration at the target locus; Figure 5). No GFP-positive parasites were detected for the ADA targeting-transfection, and so no further work was performed for this gene target.

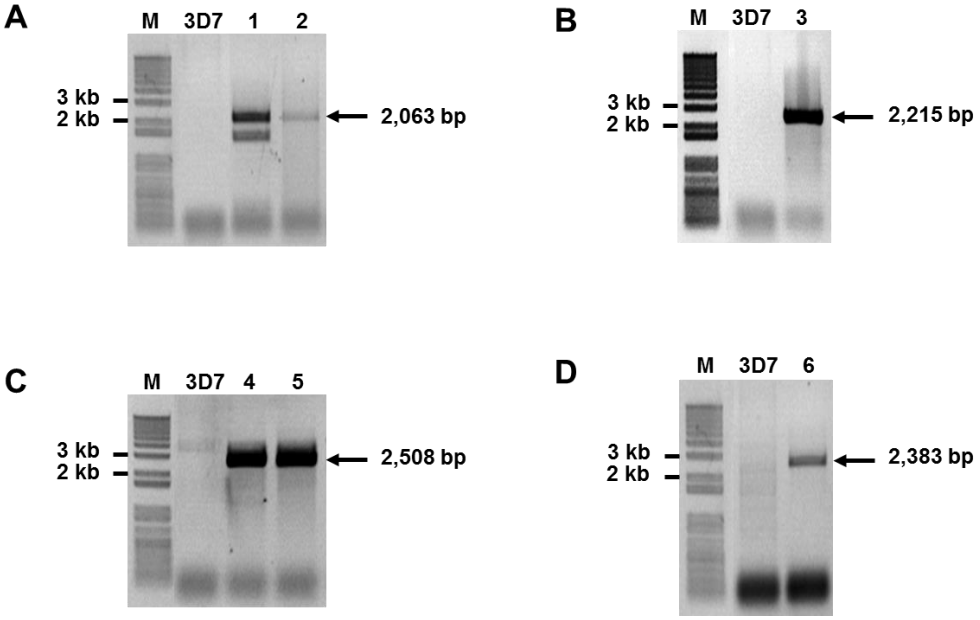

Figure 4. PCR assay to detect integration at target genes.

Samples were taken from cultures of transfected parasites after two rounds of on/off selection for integrants. Parasite genomic DNA was extracted from the parasite cultures in experiments targeting the ADA (A), CS (B), DHS (C), and TRXR (D) genes, and from *P. falciparum* 3D7 control parental parasite. (A) Integration-specific products of the expected size (2,063 bp) were observed in lanes 1 and 2 for transfection experiments Sim-pGFP-M9-ADA and Sim-pGFP-glmS-ADA, respectively. (B) An integration-specific product of the expected size (2,215 bp) was observed in lane 3 for Sim-pGFP-glmS-CS-hDHFR. (C) Integration-specific products of the expected size (2,508 bp) were observed in lanes 4 and 5 for Sim-pGFP-glmS-DHS and Sim-pGFP-M9-DHS. (D) An integration-specific product of the expected size (2,383 bp) was observed in lane 6 for Sim-pGFP-glmS-TRXR-hDHFR.

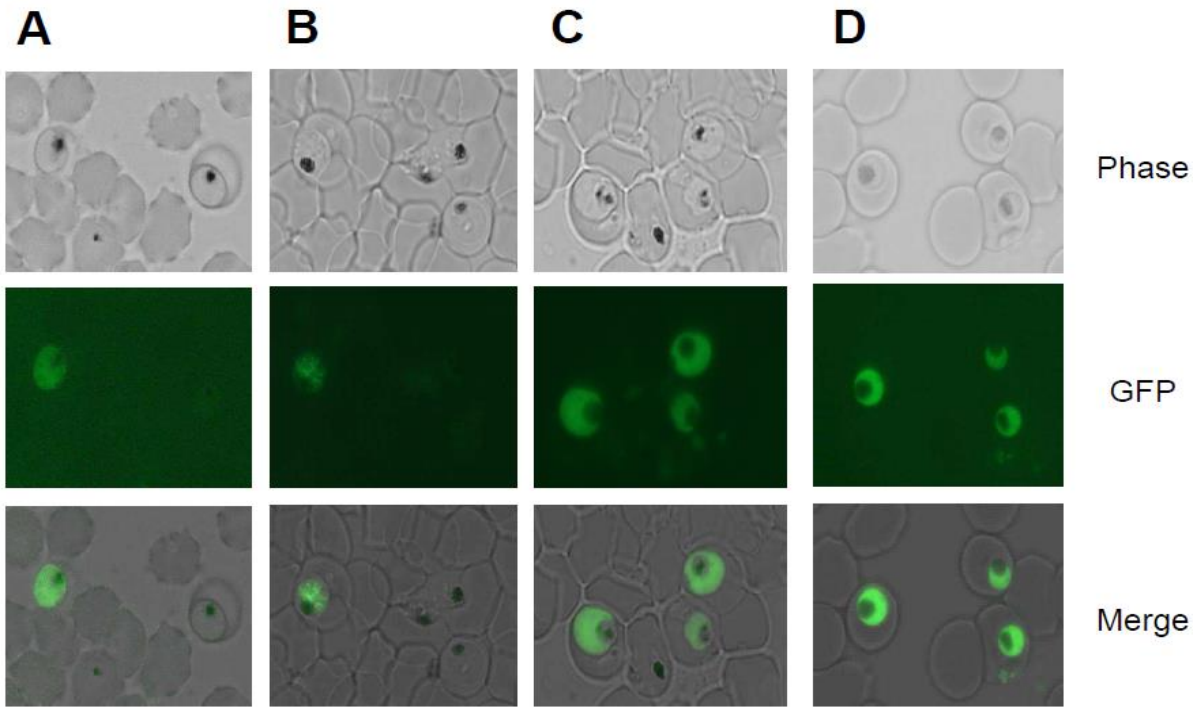

Figure 5. Fluorescence microscopy images of transgenic parasites obtained after selection.

Examples of fluorescent parasites are shown from transfection experiments using constructs Sim-pGFP-glmS-DHS (A), Sim-pGFP-glmS-CS-hDHFR (B), Sim-pGFP-glmS-TRXR-hDHFR (C) and pJRTS_GFP_glmS (D), indicating gene-targeting integration at CS, DHS, TRXR, DHFR-TS genes, respectively. The pJRTS_GFP_glmS plasmid (Prommana et al., 2013) was transfected into the K1 strain, whereas the others were transfected into the 3D7 reference strain. The top panels show phase-contrast images of parasitized red cells, the middle panels show fluorescence using filter sets for GFP, and the bottom panels the merged phase-contrast and fluorescence images.

Cloning by limiting dilution was attempted for transfected parasites with evidence of integration at target loci (Figure 4 and Figure 5). Clonal lines were established for transfections of the Sim-pGFP-glmS-DHS (functional ribozyme) and Sim-pGFP-M9-DHS (inactive ribozyme control) plasmids targeting the DHS gene. All clonal parasites for the Sim-pGFP-glmS-TRXR-hDHFR transfection targeting the TRXR gene were found to be wild-type background and not transgenic integrants. A clonal integrant line was obtained for Sim-pGFP-glmS-CS-hDHFR, but we could not detect target protein expression by fluorescence microscopy or western blot (data not shown). Therefore, we did not continue further work with this transgenic parasite as we could not determine if the expression of the CS gene can be attenuated using the *glmS* ribozyme system. Phenotypic studies were performed with the clonal lines of transgenic parasites bearing integration of *glmS* ribozyme at the DHS and DHFR-TS genes. These studies included confocal microscopic analysis of live transgenic parasites and protein analysis of target gene expression in parasites treated with *glmS* ribozyme inducer GlcN (Winkler et al., 2004), (Prommana et al.,

2013). The transgenic modifications also included insertion of GFP sequence so that parasites express a C-terminal GFP fusion protein. The GFP moiety facilitates target protein analysis. Confocal microscopic analysis showed that the GFP signal was markedly lower for the clonal parasites with integration at the DHS locus compared with the DHFR-TS locus (Figure 6).

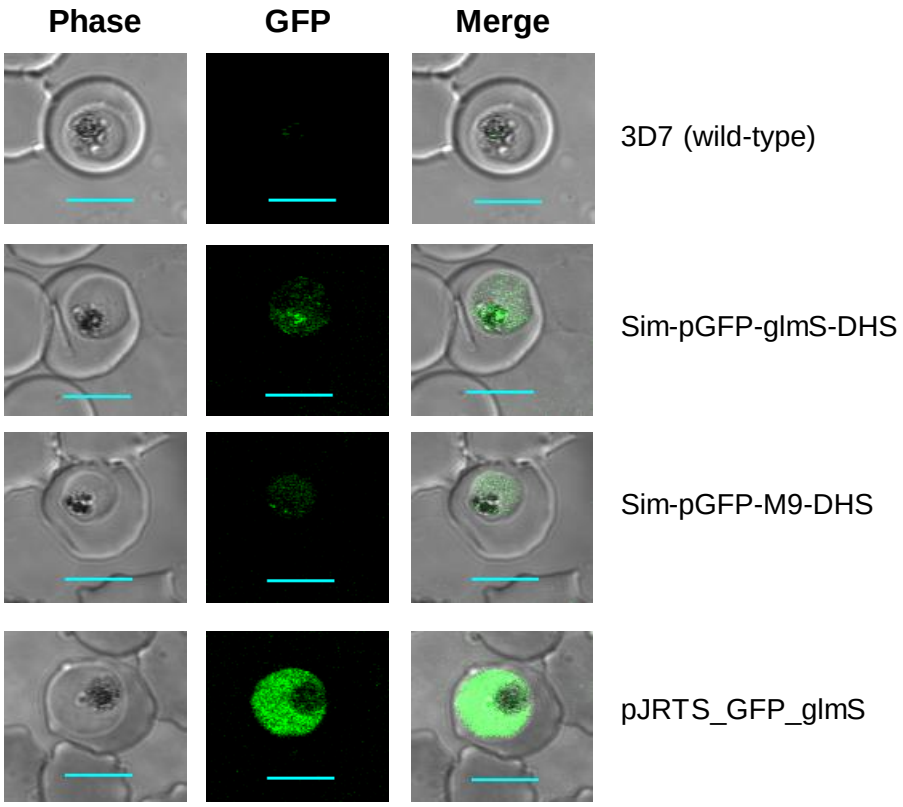

Figure 6. Confocal microscopic analysis of live parasites from integrant transgenic lines

Examples of GFP-fluorescent parasites are shown from transfection experiments using constructs Sim-pGFP-glmS-DHS, Sim-pGFP-M9-DHS and pJRTS_GFP_glmS. The 3D7 wild-type strain was the recipient for transgenic experiments with Sim-pGFP-glmS-DHS and Sim-pGFP-M9-DHS, and acts as a non-fluorescent (negative) control. The K1 strain was used as a recipient for transgenic experiments with pJRTS_GFP_glmS. The left panels show phase-contrast images of parasitized red cells, the middle panels show fluorescence using filter sets for GFP, and the right panels the merged phase-contrast and fluorescence images. Scale bars in each image represent 5 microns.

4.3 Attenuation of target gene expression in integrant transgenic parasites

Attenuation of the target gene expression in clonal lines of parasites with integration of transgenic DNA response to GlcN was measured using two protein analytical methods. Flow-cytometric enumeration of GFP-fluorescent parasites showed that the DHFR-TS target gene in K1 strain background can be attenuated by GlcN treatment, with an effective concentration of GlcN

giving rise to 50% attenuation (EC_{50}) of approximately 0.4 mM (Figure 7A). The control of DHFR-TS expression is thus very similar to the previous report for the same gene expressed in the 3D7 strain background (Prommana et al., 2013). The attenuation of target gene expression was also studied by western blotting using an anti-GFP antibody. These experiments showed that a protein band of the expected size of DHFR-TS-GFP-fusion protein was attenuated in GlcN-treated parasites (Figure 7B), in agreement with the flow cytometry analysis.

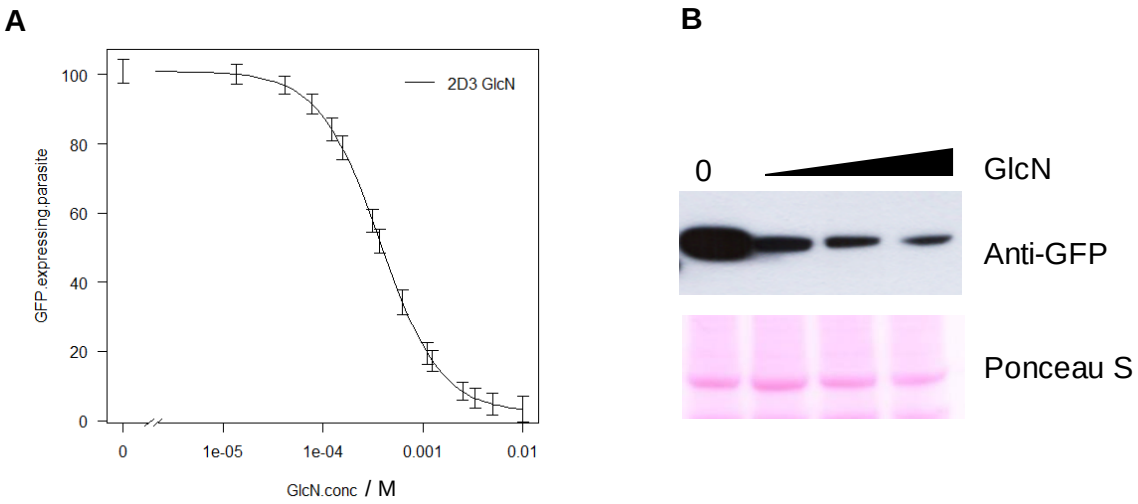

Figure 7. Attenuation of DHFR-TS-GFP target expression

DHFR-TS-GFP target protein was analysed in transgenic parasite clone 2D3 with integration of construct pJRTS_GFP_glmS in the K1 strain background. A) GFP-fluorescent parasites in ring-synchronized cultures treated with varying concentrations of GlcN (up to 10 mM) for 24 h were enumerated by flow cytometry. The numbers of GFP-positive cells were normalized to the untreated sample, which was set as 100 %. The graph shows the curve fit to the four-parameter logistic dose response equation using the drc package in R (Ritz and Streibig, 2005). The error bars represent the Bayesian-modeled errors from triplicate experiments. B) Western blot analysis using anti-GFP polyclonal antibody. Ring-stage synchronous parasites were treated with 0, 1.25, 2.5 or 5 mM GlcN for 24 h (increasing concentrations indicated by the wedge above the lanes). 18.5 µg of crude soluble protein extract was loaded in each lane. Equal loading was verified by Ponceau-S staining of the membrane after transfer (bottom panel). The signal of DHFR-TS-GFP target fusion protein migrating at approx. 100 kDa is shown in the upper panel.

The attenuation of DHS target gene was studied in the clonal transgenic lines by western blotting. Parasites with integration of Sim-pGFP-glmS-DHS carry the wild-type ribozyme, which can be activated by GlcN. This line is referred to hereafter as DHS_*glmS*. In contrast, parasites with integration of Sim-pGFP-M9-DHS bear the mutated ribozyme sequence (M9 variant), which is expected to be inactive (Winkler et al., 2004). This line is referred to hereafter as DHS_M9. The expression of DHS was strongly attenuated by GlcN treatment in DHS_*glmS* parasites, with

approximately 80% attenuation observed at 5 mM GlcN (Figure 8). In contrast, DHS expression was unaffected by GlcN treatment in the control DHS_M9 parasite (Figure 8).

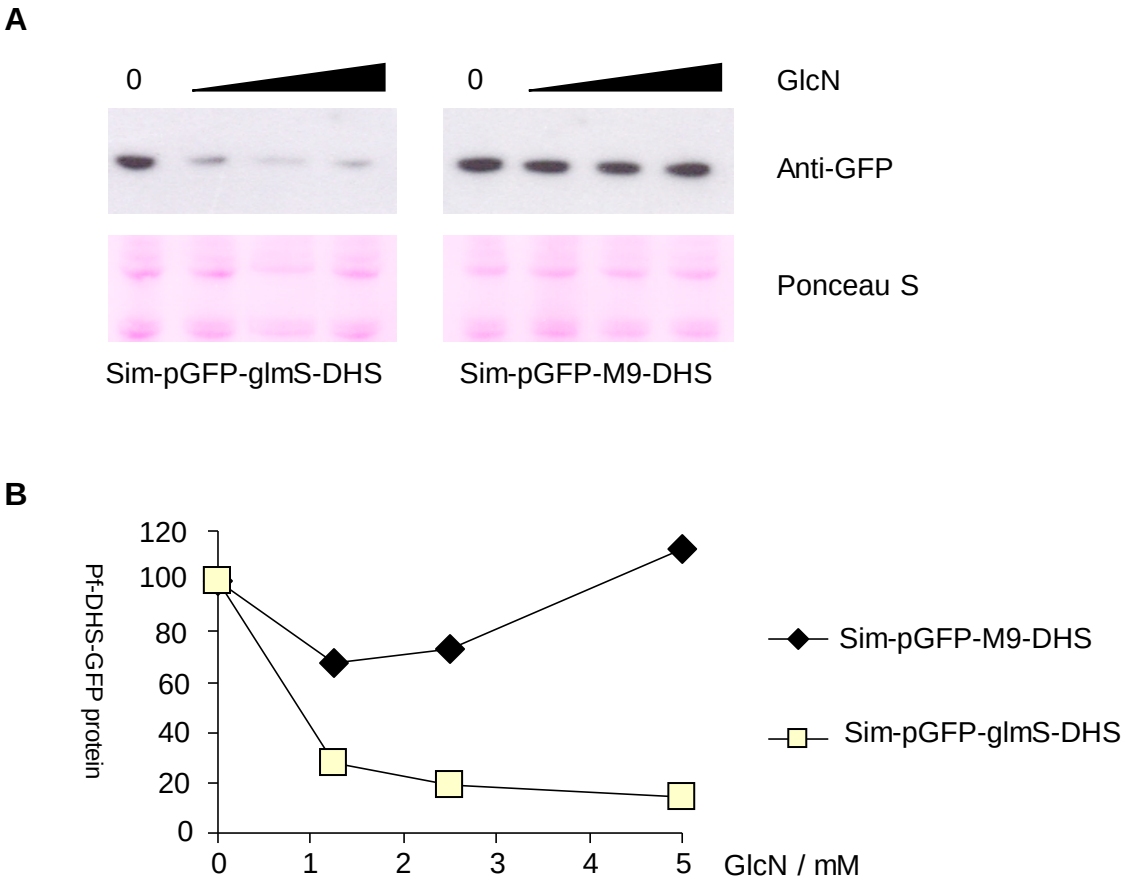

Figure 8. Attenuation of DHS-GFP target expression in clonal transgenic parasites

DHS-GFP target protein was analyzed in clonal transgenic parasites with integration of construct Sim-pGFP-glmS-DHS (active ribozyme) and construct Sim-pGFP-M9-DHS (inactive mutant) in the 3D7 strain background. A) Western blot analysis using anti-GFP polyclonal antibody. Ring-stage synchronous parasites were treated with 0, 1.25, 2.5 or 5 mM D-glucosamine for 24 h (increasing concentrations indicated by the wedge above the lanes). 7.5 µg of crude soluble protein extract was loaded in each lane. Equal loading was verified by Ponceau-S staining of the membrane after transfer (bottom panel). The signal of DHS-GFP target protein migrating at approx. 80 kDa is shown in the upper panel. B) Quantified results from Western blot analysis of DHS-GFP. The points are the average from two experiments. The intensity of the DHS-GFP band was measured by densitometry from the scanned image of the exposed X-ray film using the Image J program (Schneider et al., 2012). The protein band signals were normalized to the untreated sample, which was set as 100 %.

4.4 Growth of parasites with attenuated expression of essential genes

Following demonstration that the expression of targeted genes could be attenuated in integrant transgenic parasites (section 4.3), the effect of attenuating these putatively essential

genes on growth was studied. It was hypothesized that if the targeted genes are essential, significant growth inhibition would be observed following GlcN treatment compared with untreated parasites. It was anticipated that for some essential genes, cell cycle progression may only require a very small level of gene activity. Therefore, the incomplete attenuation of expression using conditional tools such as our ribozyme system may not be sufficient to cause a significant growth defect over a short assay period. However, if the growth assay can be extended over several cycles, we hypothesize that a cumulative growth defect can be detected. A major difficulty in performing extended growth inhibition assays is that the ribozyme-activating ligand (GlcN) has some inhibitory effect on growth by itself at the concentrations needed to significantly attenuate target gene expression. Furthermore, this confounding effect could vary depending on the culture conditions. In particular, transgenic parasites must be maintained using a drug selective regimen (blasticidin S), otherwise they can be outgrown by wild-type revertants. The transgenic selective regimen could modulate the growth inhibitory effect of the ligand, which is a concern especially for extended growth inhibition assays. To account for the confounding effect of the ligand, a control transgenic parasite is needed.

The *Pf*FC-*glmS* transgenic parasite (kindly provided by Ms. Navaporn Posayapisit, BIOTEC, Thailand) was selected as a control parasite. This parasite line has the *glmS* ribozyme element integrated at the ferrochelatase (FC) encoding gene, PF3D7_1364900. This gene is not essential, since the growth of transgenic parasites with knockout of this gene is not significantly different from wild-type in blood stages (Ke et al., 2014), (Sigala et al., 2015). Moreover, the *Pf*FC-*glmS* parasite has the same strain background (3D7) and transgenic selectable marker (BSD) as the DHS_*glmS* and DHS_M9 lines described in section 4.2. The growth of a test transgenic line with *glmS* ribozyme element integrated at a putative essential gene can be compared with that of the *Pf*FC_*glmS* control. In this manner, extended growth assays can be conducted with the confounding effects of the inducer and transgenic selective agent accounted for. Furthermore, the control and test transgenic lines can be co-cultured and the relative growth of test parasite read out as the ratio of test:control parasite. In order to determine the ratio of test:control parasites at each time-point of the growth assay, a method is needed to quantify each parasite line in co-culture. Quantitative PCR (qPCR) assays were developed with primers specific to each parasite. No product was obtained for the discriminatory amplicons TS-GFP, DHS-GFP, FC-GFP from the 3D7 parental parasite control (Figure 9). The TS-GFP amplicon thus can be used to detect and quantify clonal transgenic parasite *Pf*DHFR-TS-*glmS* (Prommana et al., 2013), the DHS-GFP amplicon for *Pf*DHS_*glmS* and *Pf*DHS_M9 parasites, and the FC-GFP amplicon for *Pf*FC-*glmS* parasites. Experiments with titration of template DNA showed that all primers had comparable efficiency, and so were validated for qPCR (Table 3).

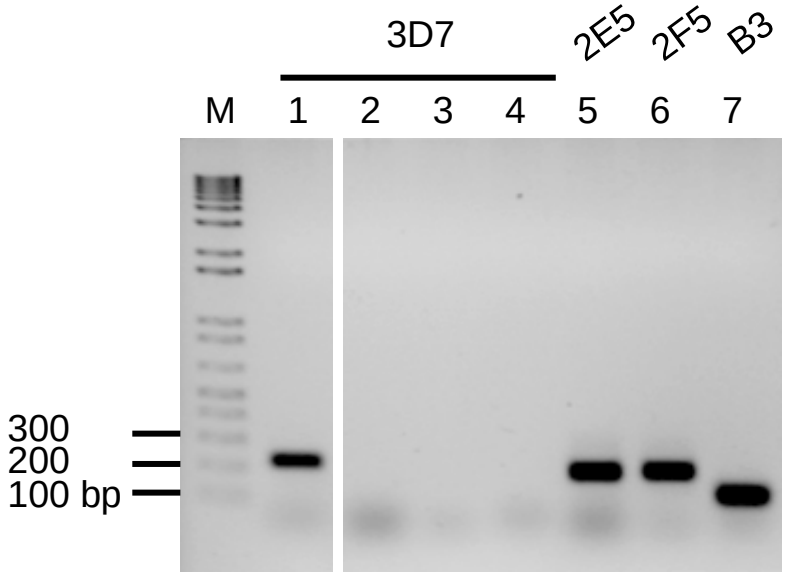

Figure 9. Agarose gel analysis of qPCR amplicons.

Amplicons were separated in 2% agarose gel and stained with ethidium bromide. Genomic DNA templates used in each analysis are shown above the gel: 3D7, parental wild-type parasite; 2F5, clonal transgenic parasite *Pf*DHFR-TS-*glmS* (Prommana et al., 2013); 2E5, clonal transgenic *Pf*DHS_*glmS*; B3, clonal transgenic parasite *Pf*FC-*glmS*. Lane M is 1 Kb plus DNA ladder (Invitrogen). Tested amplicons in lanes 1 to 7 are LDH, TS-GFP, DHS-GFP, FC-GFP, TS-GFP, DHS-GFP, and FC-GFP, respectively (see Table 3 for details of amplicons).

After validating qPCR primer efficiency and specificity, qPCRs were conducted using purified genomic DNA templates mixed in different ratios to validate the method for quantifying parasite ratios. Genomic DNA was obtained from the *Pf*DHFR-TS-*glmS* (Prommana et al., 2013), *Pf*DHS_*glmS* and *Pf*FC-*glmS* parasites. The genomic DNAs were quantified by Nanodrop and mixed in different ratios according to the measured DNA concentrations. Quantification cycles (Cq) for each transgenic-integration specific amplicon (DHS-GFP, TS-GFP and FC-GFP) were transformed and normalized to LDH to give measurements of gene target abundance. The observed ratios of gene abundance from qPCR data were plotted against expected ratios, and highly significant linear correlations were observed (Figure 10). From these experiments, we were confident that the qPCR assay can be used to assess relative growth of co-cultured transgenic parasites.

Table 3. Target genes and details of PCR primers for qPCR

Target gene and purpose	*Amplicon symbol*	*Forward primer 5′—3′*	*Reverse primer 5′—3′*	*Amplicon size (bp)*	*PCR efficiency (%)*	*Coefficient of linear regression (R^2)*
PF3D7_1324900 (L-lactate dehydrogenase); normalizing gene for template DNA input	LDH	GCACCAAAAGCAAAAATCGT	ACATCTGCTCCAGCCAAATC	221	101	0.997
PF3D7_0417200 (dihydrofolate reductase thymidylate synthase); integration-specific amplicon	TS-GFP	ACCCTATCCATTCCCAACAC	TGGGACAACTCCAGTGAAAA	190	96	0.998
PF3D7_1412600 (deoxyhypusine synthase); integration-specific amplicon	DHS-GFP	TTTGGTGATGCAACCATTTT	TTGTGCCCATTAACATCACC	188	103	0.996
PF3D7_1364900 (ferrochelatase); integration-specific amplicon	FC-GFP	AATATAATAGGATGGGTGTCAGG	TTGTGCCCATTAACATCACC	125	102	0.993

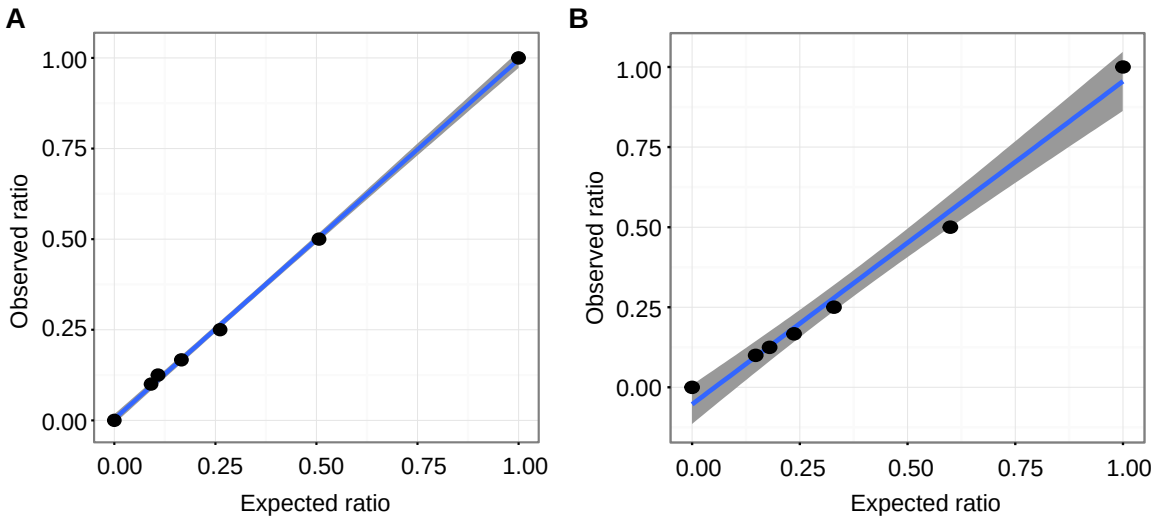

Figure 10. Validation of qPCR assay for measuring ratios of genomic DNA from transgenic parasites.

Purified genomic DNA samples from each parasite were mixed in various ratios according to Nanodrop measurements of DNA concentrations. The qPCR abundances of DHS-GFP, TS-GFP and FC-GFP amplicons were normalized to the LDH amplicon and were used to calculate DNA ratios. The Pearson's coefficient of correlation of observed ratios from qPCR data and expected ratios from known DNA concentration was calculated in R.

A. Correlation of observed and expected ratio of *Pf*DHS_*glmS* and *Pf*FC-*glmS* genomic DNA (Pearson's r=0.9996; *P*=4.15 e-09). CI_{95} for linear fit are shaded in gray.
B. Correlation of observed and expected ratio of *Pf*DHFR-TS_GFP_*glmS* and *Pf*FC-*glmS* genomic DNA (Pearson's r=0.9939; *P*=5.59e-06). CI_{95} for linear fit are shaded in gray.

Growth inhibition assays were conducted by co-culturing synchronized ring-stage test transgenic parasite with *Pf*FC-*glmS* control transgenic parasite. Co-cultures were treated with GlcN and parasite samples were taken every two growth cycles until the tenth growth cycle. Blasticidin-S was added to maintain selection of transgenic parasites. The data show that the *Pf*DHFR-TS_*glmS* parasite growth is markedly reduced by GlcN treatment, even as early as the second growth cycle, in agreement with (Prommana et al., 2013). The growth of the DHS_*glmS* parasite also appears to be inhibited by GlcN, although the inhibition is marked only for the 5.0 mM GlcN treatment compared with untreated parasites. The effect of GlcN on growth over time is significant for the *Pf*DHFR-TS_*glmS* and DHS_*glmS* parasites. In contrast, GlcN has no significant effect on growth of the DHS_M9 parasite (Figure 11).

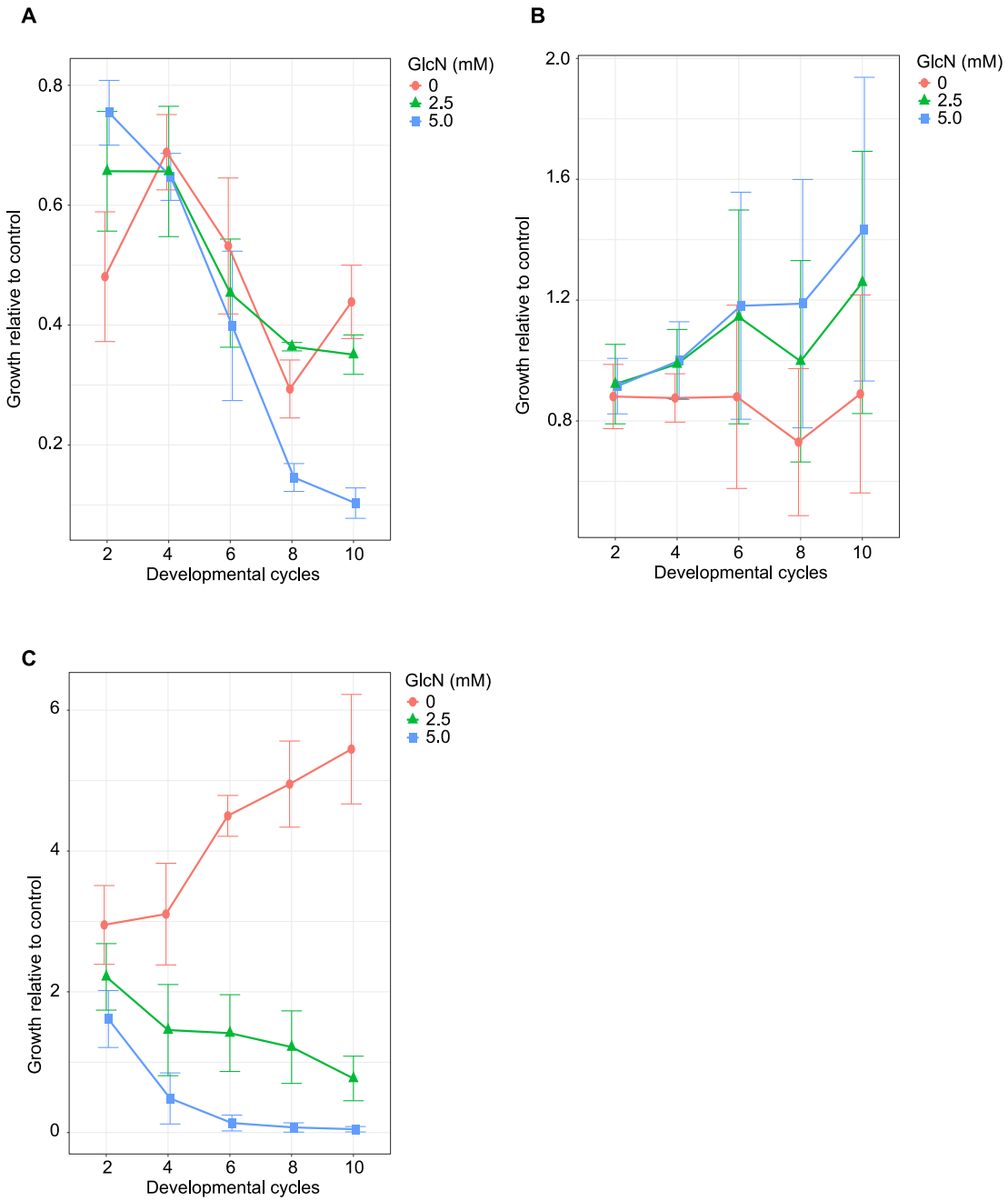

Figure 11. Transgenic parasite co-culture growth inhibition assay.

*Pf*FC_*glmS* was used as a control parasite for assessing growth of other transgenic parasites. Co-cultures of *Pf*FC_*glmS* with *Pf*DHFR-TS_*glmS*, DHS_*glmS* or DHS_M9 parasites were established. Cultures were treated with 0, 2.5 or 5.0 mM GlcN. Parasite samples were taken from cultures at the trophozoite stage every two growth cycles (96 h) until the tenth growth cycle (21 days). Genomic DNA was extracted and purified from parasite samples, and the genomic DNA was used as a template in qPCR assays. The ratio of the test transgenic parasite to the control *Pf*FC_*glmS* was determined from the normalized abundance of the test amplicon (TS-GFP or DHS-GFP) relative to the FC-GFP amplicon. The test parasite ratio was taken as the measure of growth relative to control (*Pf*FC_*glmS*). The points shown on each graph are the mean of three independent experiments; error bars represent standard errors. Statistical analysis of growth was performed by linear mixed effect modeling of the data. Likelihood ratio test results of null model (growth varies as a function of time) vs full model (growth varies as a function of time with GlcN as a fixed effect): *Pf*DHFR-TS_*glmS*, P=0.00003; DHS_*glmS*, P=0.02; DHS_M9, P=1.

4.5 Chemogenomic profiling identifies antimalarial mode of action

The demonstration that attenuation of expression of the putative essential genes DHFR-TS and DHS leads to a growth defect in integrant transgenic parasites (section 4.4) validates these genes as antimalarial drug targets. We selected the K1_GFP_DHFRTS_*glmS* integrant line for phenotypic study (section 4.3) together with the 3D7_GFP_DHFRTS_*glmS* transgenic line bearing modification of the same gene, but in the 3D7 strain background (Prommana et al., 2013). The DHFR-TS gene expression is attenuated with similar efficiency in these parasites using the ribozyme system (section 4.3). The K1 and 3D7 strains differ in their sensitivity to antifolate antimalarials, in which the K1 strain is much less sensitive owing to resistance mutations in the DHFR-TS gene (Foote et al., 1990). We hypothesized that attenuation of DHFR-TS expression in these transgenic lines would sensitize them to antifolate antimalarials known to target DHFR-TS, but not other drugs with different mode of action (MoA). This rationale is the basis for chemogenomic profiling (reviewed in (Nijman, 2015)). By testing in two different strains, we can determine the robustness and reproducibility of the chemogenomic profiling method. Chemogenomic profiling was performed by dose-response assays to determine effective concentrations of compound that inhibit growth by 50% (EC_{50}). For these assays, parasites were cultured in the presence of varying concentrations of antimalarial compound. The growth was assessed flow cytometry or fluorescence plate reader (Smilkstein et al., 2004). Dose-response assays were performed with (+GlcN) or without (-GlcN) co-treatment with 2.5 mM D-glucosamine. In the +GlcN condition, expression of DHFR-TS is attenuated approximately five fold in both transgenic lines with insertion of *glmS* ribozyme at DHFR-TS (section 4.3). The EC_{50} values determined from both conditions were used to calculate $\log_2$ ratios of EC_{50} values (−GlcN/+GlcN). If the compound targets the gene with attenuated expression, parasites are sensitized to the compound and the $\log_2$ EC_{50} ratio will be significantly greater than zero.

Chemogenomic profiling proof of concept was demonstrated with antimalarial drugs (Figure 12). The $\log_2$ EC_{50} (−GlcN/+GlcN) ratios are significantly greater than zero for the transgenic *P. falciparum* parasites 3D7_ GFP_DHFRTS_*glmS* and K1_ GFP_DHFRTS_*glmS* with modification of the DHFR-TS gene exposed to antifolate antimalarial drugs known to target DHFR-TS, i.e. PYR, methotrexate (MTX), cycloguanil (CYC) and WR99210. In contrast, the $\log_2$ EC_{50} ratios for other antimalarial that do not target DHFR-TS (dihydroartemisinin (DHA), atovaquone (ATQ), proguanil (PGN) and DSM1; MoA of each reviewed in (Flannery et al., 2013)) are not significantly greater than zero. For the control parental strains 3D7 and K1, the $\log_2$ EC_{50} ratios are not significantly greater than zero for any of the antimalarials tested. We infer from these data that parasites with attenuated DHFR-TS expression are sensitized to drugs specifically targeting DHFR-TS. Interestingly, although the $\log_2$ EC_{50} ratio for the K1_

GFP_DHFRTS_*glmS* parasite exposed to PYR is significant, the ratio is approximately two-fold lower than that of the 3D7_GFP_DHFRTS_*glmS* parasite exposed to the same drug.

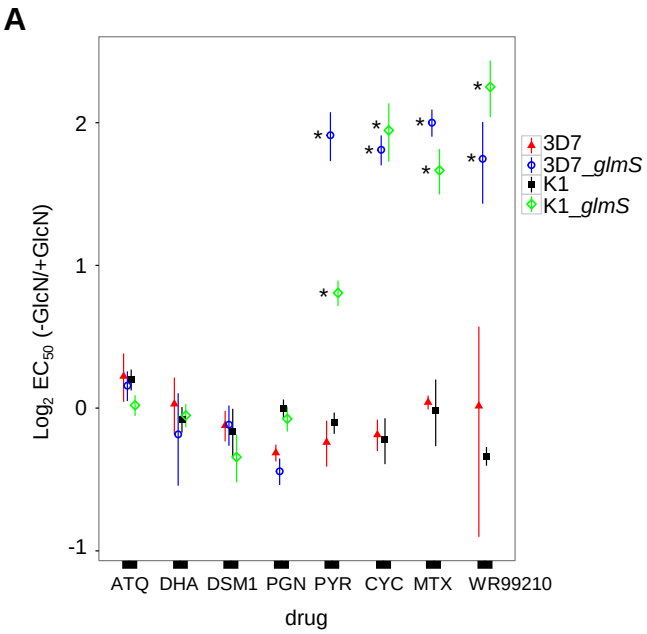

Figure 12. Chemogenomic profiling identifies DHFR-TS as the target of antifolate antimalarials in vivo.

Cultures of *Plasmodium falciparum* parasites were established in 96-well plates. Wells contained varying concentrations of antimalarial compound, which were supplemented with 2.5 mM glucosamine (+GlcN), or without (-GlcN). Growth of parasites over 48 h at 37°C was measured by staining parasitized cells with SYBR Green I and enumerating by flow cytometry (Prommana et al., 2013). The concentration of compound producing 50% growth inhibition (EC_{50}) was calculated from the data. The parasites tested included parental strains 3D7 (pyrimethamine (PYR) sensitive) and K1 (PYR resistant), and transgenic lines 3D7_ GFP_DHFRTS_*glmS* (indicated as 3D7_*glmS*) and K1_ GFP_DHFRTS_*glmS* (indicated as K1_*glmS*). The transgenic lines have modification of the *Pf*DHFR-TS gene, the expression of which is attenuated approximately five-fold by 2.5 mM GlcN co-treatment. The data were obtained from three to seven independent experiments. The antimalarial drugs tested include Atovaquone (ATQ), PYR, cycloguanil (CYC), WR99210, dihydroartemisinin (DHA), proguanil (PGN), DSM1, and methotrexate (MTX). The $\log_2 EC_{50}$ (-GlcN/+GlcN) ratios that are significantly greater than zero (*F*-test $P < 0.001$) are indicated by asterisks. Error bars represent standard errors of estimated ratios.

The chemogenomic profiling approach was used for identifying novel inhibitors of DHFR-TS. The Malaria Box compound library containing 400 compounds of diverse chemical scaffolds, available from the Medicines for Malaria Venture (MMV), Switzerland (Spangenberg et al., 2013), was screened using the 3D7_GFP_DHFRTS_*glmS* parasite. This work was performed in collaboration with our colleagues at the BIOTEC institute (Thailand), Dr. Chairat Uthaipibull, Dr.

Sumalee Kamchonwongpaisan and Ms. Navaporn Posayapisit. Two compounds from this library (MMV667486 and MMV667487) were identified as DHFR-TS inhibitors, with $\log_2$ EC_{50} ratios similar to pyrimethamine (Figure 13).

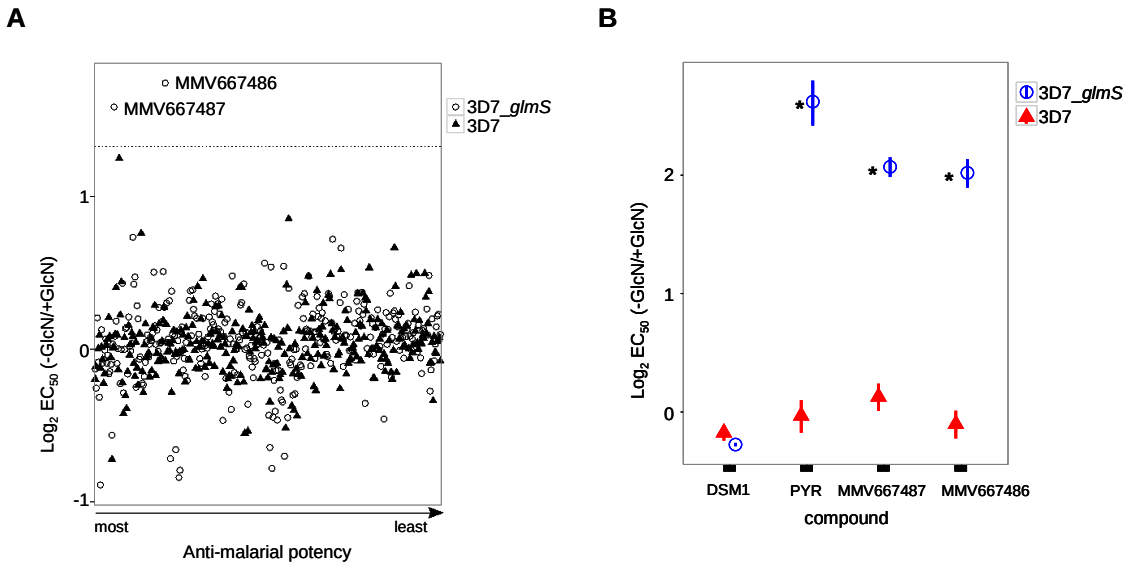

Figure 13. Chemogenomic profiling identifies novel inhibitors of DHFR-TS.

Cultures of *Plasmodium falciparum* parasites were established in 96-well plates. Wells contained varying concentrations of antimalarial compound, which were supplemented with 2.5 mM glucosamine (+GlcN), or without (-GlcN). Growth of parasites over 48 h at 37°C was measured by staining parasitized cells with SYBR Green I and enumerating by fluorescence plate reader (Smilkstein et al., 2004). The concentration of compound producing 50% growth inhibition (EC_{50}) was calculated from the data. The parasites tested included parental strains 3D7 (pyrimethamine (PYR) sensitive) and transgenic line 3D7_GFP_DHFRTS_*glmS* (indicated as 3D7_*glmS*).

A. Medium-throughput screening of the Malaria Box compound library. The compound data points are sorted according to antimalarial potency (EC_{50} values reported by the Medicines for Malaria Venture). The dashed line indicates the threshold of EC_{50} ratio for identifying hit compounds targeting DHFR-TS, which is defined as the mean EC_{50} ratio of 311 compounds tested against the 3D7_*glmS* parasite plus six standard deviations. The two compound hits MMV667486 and MMV667487 are indicated on the plot.

B. Re-testing of EC_{50} ratios to confirm novel DHFR-TS targeting compounds. Growth inhibition of *P. falciparum* parasites was measured as in part A. The $\log_2$ EC_{50} ratios were determined from triplicate experiments and the error bars represent standard errors. The $\log_2$ EC_{50} values that are significantly greater than zero (*F*-test $p<0.001$) are indicated by asterisks. Control compounds for comparison include DSM1 (an inhibitor of DHODH; (Phillips et al., 2008)), and pyrimethamine, a known inhibitor of DHFR-TS (Yuvaniyama et al., 2003).

Next, having demonstrated that the chemogenomic profiling approach can identify DHFR-TS as the target of antifolate drugs and structurally related compounds in vivo, we took the same

approach for identifying compounds that target DHS (Figure 14). Integrant transgenic parasites DHS_*glmS* (active ribozyme) and DHS_M9 (inactive mutated ribozyme control) were used for chemogenomic profiling. Chemogenomic profiling was performed with these transgenic parasites and different antimalarial compounds. Growth inhibition was measured by dose-response assays with (+GlcN) or without (-GlcN) 2.5 mM GlcN co-treatment, and EC_{50} values were calculated from the data. The $\log_2$ EC_{50} (-GlcN/+GlcN) ratios for pyrimethamine and cycloheximide that are known not to target DHS were not significantly greater than zero in either parasite, as expected. Compound N1-guanyl-1,7-diaminoheptane (GC7) is described as a potent inhibitor of DHS enzymes in different organisms. Chemogenomic profiling of GC7 compound showed a $\log_2$ EC_{50} (-GlcN/+GlcN) ratio significantly greater than zero for the DHS_*glmS* parasite, but not the DHS_M9 parasite. Interestingly, the $\log_2$ EC_{50} (-GlcN/+GlcN) ratio is only 0.45 for GC7 against the DHS_*glmS* parasite.

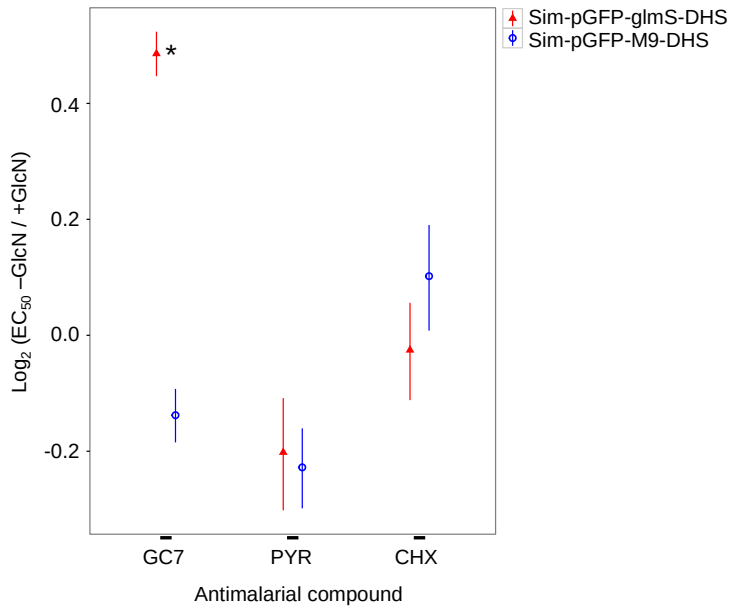

Figure 14. Chemogenomic profiling identifies DHS as the target of compound GC7.

Cultures of *Plasmodium falciparum* parasites were established in 96-well plates. Wells contained varying concentrations of antimalarial compound, which were supplemented with 2.5 mM glucosamine (+GlcN), or without (-GlcN). Growth of parasites over 48 h at 37°C was measured by staining parasitized cells with SYBR Green I and enumerating by flow cytometry (Prommana et al., 2013). The concentration of compound producing 50% growth inhibition (EC_{50}) was calculated from the data. The parasites tested included transgenic lines Sim_ pGFP_*glmS*_DHS (DHS_*glmS*, active ribozyme) and Sim_ pGFP_M9_DHS (DHS_M9, inactive ribozyme control). The transgenic lines have modification of the DHS gene, the expression of which can be attenuated approximately five-fold by 2.5 mM GlcN co-treatment (section 4.3). The data were obtained from three independent experiments. The antimalarial compounds tested include N1-guanyl-1,7-diaminoheptane (GC7), Pyrimethamine (PYR) and cycloheximide (CHX). The $\log_2$ EC_{50} (-GlcN/+GlcN) ratio that is significantly greater than zero (*F*-test $P < 0.001$) is indicated by an asterisk. Error bars represent standard errors of estimated ratios.

4.6 Testing the effect of ribozyme regulatory element location on target gene expression

The experiments with transgenic parasites with attenuated DHFR-TS and DHS expression demonstrate the essentiality of these genes and identify antimalarials targeting these genes. Although encouraging, the *glmS* ribozyme tool may not be generally applicable to other antimalarial targets, as the degree of attenuation is limited to about 10 fold or less. The incomplete attenuation using this system may be insufficient to observe growth defects in transgenic parasites with attenuated target gene expression, or identify targets of compounds with weak antimalarial activity. The *glmS* ribozyme tool was conceived to control target gene expression when the ribozyme element is placed in the in 3′ UTR position. The *glmS* ribozyme may function more efficiently in the 5′ UTR position, since ribozyme-cleaved target mRNA would likely be less stable *in vivo* owing to loss of 5′ cap. The 5′ cap is the main determinant of eukaryote mRNA stability, since decapped mRNA is rapidly degraded by the conserved XRN1 nuclease (Meaux, 2006). The location of the ribozyme element was originally limited to the 3′ UTR position as this facilitates integration by single cross-over recombination. Integration of DNA elements in gene 5′ flanking regions is much more difficult by conventional means, requiring lengthy and inefficient negative selection (Duraisingh et al., 2002). With the advent of the Clustered, Regularly Interspaced, Short Palindromic Repeat (CRISPR)-Cas9 genome editing system in *P. falciparum* (Ghorbal et al., 2014), marker-free modifications can be made in target gene 5′ or 3′ flanking regions. However, integration of DNA elements by CRISPR-Cas9 editing is more complicated than conventional recombination and requires considerable effort in design and construction of transfection vectors. Therefore, we wished to test whether the *glmS* ribozyme can work for controlling gene expression when placed in the 5′ position through a simple experiment. Four plasmids were constructed for transfection experiments to test the effect of ribozyme location with respect to an episomally expressed reporter gene. The *glmS* ribozyme was placed in the 5′ position (p5Rbz_HAEGFP_hDHFR), the 3′ position (p3Rbz_HAEGFP_hDHFR), and both 5′ and 3′ positions (p53Rbz_HAEGFP_hDHFR). The forth plasmid, pHAEGFP_hDHFR, contains no ribozyme element and thus serves as a control. The reporter gene from the control plasmid is expected to show strong activity in transfected parasites, and its expression should not be affected by GlcN treatment.

Episomally transfected *P. falciparum* parasites were obtained for each plasmid after 3 weeks of selection with blasticidin. Reporter gene activity in the four transgenic lines was assessed by confocal microscopic imaging of live parasites. Strong reporter expression was evident in parasites transfected with control plasmid pHAEGFP_hDHFR (no ribozyme, Figure 15A) and plasmid with ribozyme in the 3′ UTR position only (p3Rbz_HAEGFP_hDHFR, Figure 15B). In contrast, reporter activity was markedly lower in parasites transfected with plasmids containing

glmS ribozyme in the 5′ UTR position (plasmids p5Rbz_HAEGFP_hDHFR, Figure 15C; p53Rbz_HAEGFP_hDHFR, Figure 15D). Quantitative analysis of GFP signals showed that under normal growth conditions, the ribozyme reduced reporter gene activity, with the 5′ position having a markedly greater effect than the 3′ position (Figure 16).

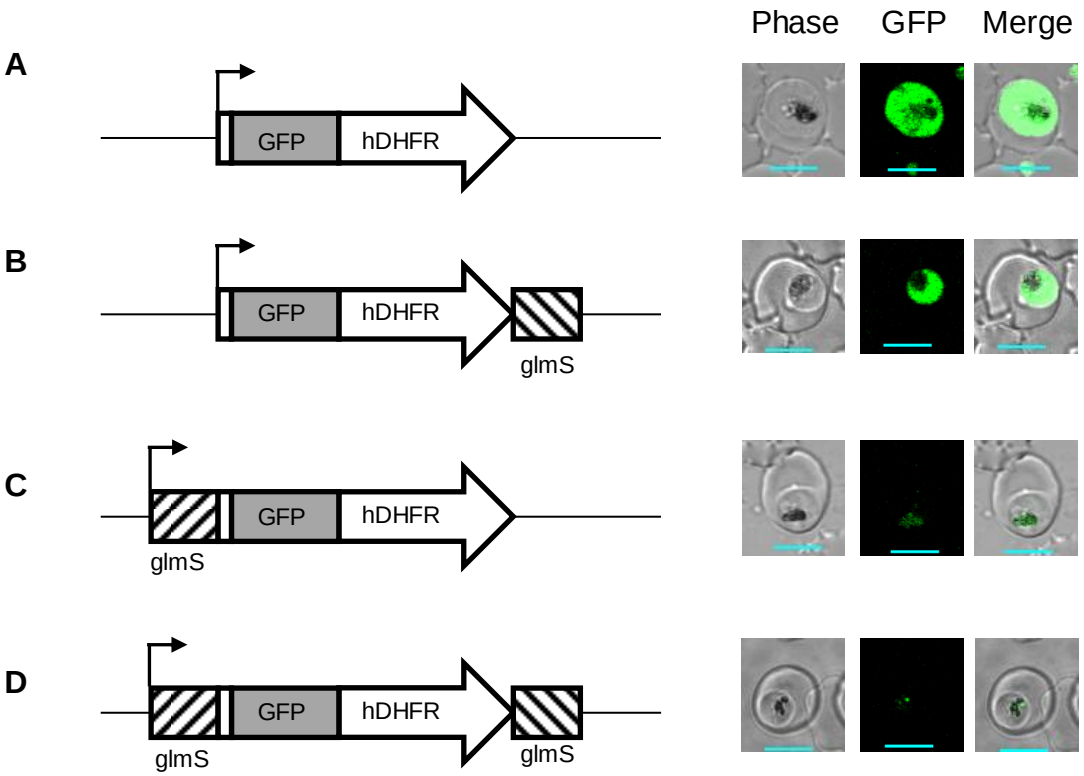

Figure 15. Confocal microscopic analysis of live parasites carrying episomal transgenic reporters.

Four plasmids A) pHAEGFP_hDHFR; B) p3Rbz_HAEGFP_hDHFR; C) p5Rbz_HAEGFP_hDHFR D) p53Rbz_HAEGFP_hDHFR were constructed and transfected into 3D7 strain *P. falciparum* parasites. For each transfected plasmid, a schematic diagram of the reporter gene expression cassette is shown. Each plasmid contains a reporter gene coding for a fusion protein with hemagglutinin (HA, white bar), green fluorescent protein (GFP) and human dihydrofolate reductase (hDHFR) moieties. The *glmS* ribozyme element is indicated by the striped box (not to scale). To the right of the schematic diagrams, images from confocal microscopic analysis are shown. The left panels show phase-contrast images of parasitized erythrocytes, the middle panels show fluorescence using filter sets for GFP, and the right panels show the merged phase-contrast and fluorescence images. Scale bars in each image represent 5 microns.

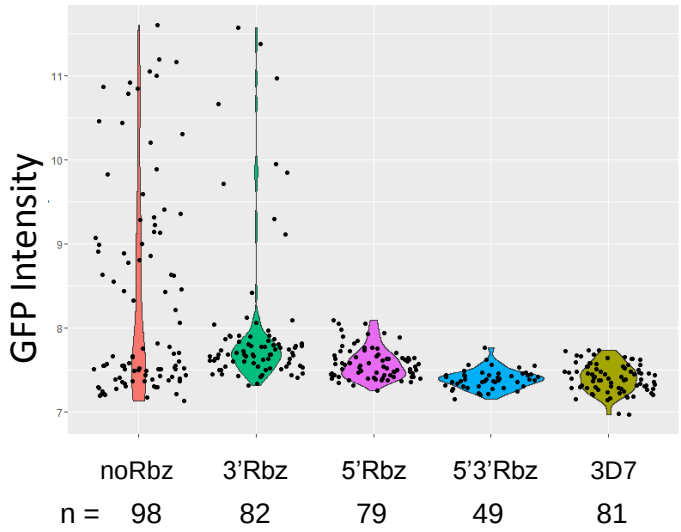

Figure 16. Quantitative analysis of GFP signals from confocal microscopy.

Fluorescence images of individual erythrocytes infected with *P. falciparum* parasites were captured using confocal microscopy with GFP filter sets. The distributions of fluorescence signal (arbitrary units) for each parasite line studied are shown as violin plots. The numbers of cells analyzed for each distribution (n) are shown below the horizontal axis. The 3D7 reference strain (labeled 3D7) was used as a non-fluorescent control. Transgenic parasites transfected with different plasmids are shown in separate columns: pHAEGFP_hDHFR (labeled noRbz); p3Rbz_HAEGFP_hDHFR (labeled 3'Rbz); p5Rbz_HAEGFP_hDHFR (labeled 5'Rbz) and p53Rbz_HAEGFP_hDHFR (labeled 5'3'Rbz). The means contrasts of each group of transgenic parasite compared with the 3D7 control are: pHAEGFP_hDHFR, 0.91; p3Rbz_HAEGFP_hDHFR, 0.57; p5Rbz_HAEGFP_hDHFR, 0.17; p53Rbz_HAEGFP_hDHFR, -0.01. All of the transgenic parasite group means are significantly greater than the 3D7 control (P<0.00001), except for p53Rbz_HAEGFP_hDHFR (P=0.98).

The control of reporter gene expression by GlcN treatment was assessed by western blotting (Figure 17). As expected, reporter gene expression was unaffected by GlcN treatment in the pHAEGFP_hDHFR control line (Figure 17A). Reporter expression was markedly attenuated in the p3Rbz_HAEGFP_hDHFR transgenic line harboring *glmS* ribozyme in the 3′ UTR position for GlcN-treated compared with untreated parasites from the same transgenic backgrounds (Figure 17B). Unexpectedly, reporter gene expression was unaffected by GlcN treatment in the p5Rbz_HAEGFP_hDHFR line harboring *glmS* ribozyme in the 5′ UTR position (Figure 17C). The reporter expression appeared to decrease in the p53Rbz_HAEGFP_hDHFR line after GlcN treatment, although since the signal was very weak in the untreated parasites, it is difficult to assess the degree of attenuation in this line (Figure 17D).

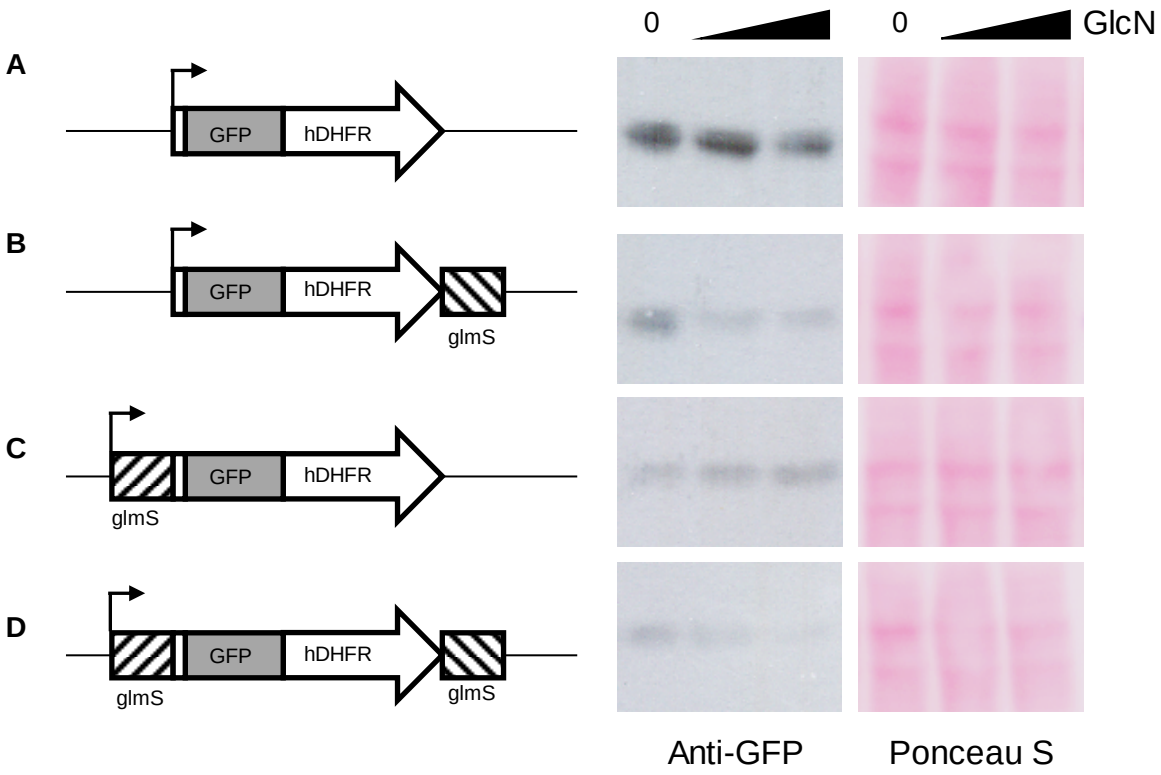

Figure 17. Control of reporter gene expression in episomally transfected transgenic parasites.

Four plasmids A) pHAEGFP_hDHFR; B) p3Rbz_HAEGFP_hDHFR; C) p5Rbz_HAEGFP_hDHFR and D) p53Rbz_HAEGFP_hDHFR were constructed and transfected into 3D7 strain parasites. Schematic diagrams of the reporter gene are shown on the left (see detail in Figure 15 legend). Ring-stage synchronous parasites were treated with 0, 2.5 or 5 mM GlcN for 24 h (increasing concentrations indicated by the wedge above the lanes). Crude soluble protein extract from 1.5 x 10^7 parasites was loaded in each lane. HA-eGFP-hDHFR target protein was detected using anti-GFP polyclonal antibody. A protein band migrating at the expected size of approx. 50 kDa was observed (panels labeled anti-GFP). Equal loading was verified by Ponceau-S staining of the membrane after transfer (far right panel).

5. Discussion and conclusions

The main objective of the project was to establish transgenic parasite lines with the *glmS* ribozyme element integrated at several candidate drug target genes. 13 candidate genes were identified from literature search as genes likely to represent essential genes and drug targets. Targeting sequences for directing homologous recombination at these genes could be obtained from 10/13 genes. The failure to PCR amplify some sequences is likely due to the high AT content of these sequences. High AT-content can limit PCR amplification, probably because of mismatching of the weaker A:T basepairs.

Plasmids were constructed for integration of DNA into ten genes, and drug-resistant parasites were obtained for all plasmids after transfection. However, integration of DNA was detected only for four genes after drug cycling to remove episomally transfected parasites. The lack of integration at some gene targets could be due to low recombination frequency. Recombination frequency in model organisms such as *S. cerevisiae* yeast is known to vary across the genome. Recombination is initiated by homologous repair of double-strand breaks in DNA, which typically occur during DNA synthesis at stalled replication forks (Raveendranathan et al., 2006). Genomic regions prone to form stalled replication forks include regions with unusual DNA structures (such as those that occur within simple sequence repeats (micro- and minisatellites) and inverted repeats, (Song et al., 2014)), and in highly transcribed genes (Azvolinsky et al., 2009). The targeted genes for which integration was not successful may lack sites of stalled replication forks, and so double-strand breaks may occur too rarely for homology repair with the transgenic DNA to be triggered. Another possible reason for failure to integrate DNA is that the modification disrupts gene function in an unexpected fashion and integrant parasites cannot grow, if the genes are essential as predicted. For gene targets in which integration is not successful because of low recombination frequency, genome editing tools such as CRISPR-Cas9 (Ghorbal et al., 2014) could be useful. Recently, the CRISPR-Cas9 tool was used to integrate the *glmS* ribozyme into the essential RhopH2 and RhopH3 genes; integrant parasites were obtained within 3 weeks post-transfection (Ito et al., 2017). As an alternative to genome editing tools, integration of transfection DNA has been reported to occur more efficiently in *P. falciparum* using the selection-linked integration method, in which integrants can be positively selected using a marker gene that is active only in integrants (Birnbaum et al., 2017).

Although integration was detected at the ADA gene by PCR, no GFP fluorescent parasites were observed. The lack of fluorescent parasites was unexpected, since the ADA protein is of high abundance, according to the available ribosome profiling data published in (Caro et al., 2014). Ribosome profiling is an indirect measure of protein abundance based on ribosome footprint density. For comparison, the early trophozoite ribosome occupancy for the endogenous

ADA gene is about ten times greater than DHFR-TS (Caro et al., 2014). The DHFR-TS protein is of moderate abundance, and is readily detectable and quantifiable by different methods (see section 4.3). Without further evidence, including sequence data of the integrated ADA gene, we cannot speculate as to the reason why the protein cannot be detected. Integration was detected at the TRXR gene, and GFP fluorescent parasites were observed suggesting that modification of this gene can be tolerated. However, clonal lines could not be obtained. The failure to isolate clones of TRXR integrants may be due to a growth defect, if the ribozyme affects the normal expression of this gene even in the absence of GlcN inducer. This phenomenon is referred to as the roof gap, in which the maximal level of gene expression is lower in transgenic parasites with modified genes (Aroonsri et al., 2016). Clonal lines of parasites with ribozyme modification of the CS gene were obtained, although no CS protein could be detected by western blotting using an anti-GFP antibody or by microscopy. A few GFP-fluorescent parasites showing a weak, but punctate signal could be detected before drug cycling (Figure 5). The CS protein is likely to be of low abundance, according to ribosome profiling data in (Caro et al., 2014); for instance, the early trophozoite ribosome ribosome occupancy for CS is about five times lower than DHFR-TS. The failure to reliably detect and quantify the CS protein prevented assessment of the attenuation of this gene's expression by the ribozyme system, and thus no conclusions could be reliably made from phenotypic studies. We were successful in obtaining integrant transgenic lines for the DHS gene, for both the active (DHS_*glmS*) and inactive (DHS_M9) ribozyme variants. Moreover, although this protein is of rather low abundance in mature stages, as shown by the weak fluorescent signals in confocal microscopy, we were able to detect and quantify it by western blotting.

The growth of transgenic integrant parasites carrying ribozyme modifications of the DHFR-TS and DHS genes were shown to be significantly inhibited after GlcN treatment (Figure 11). The degree of growth inhibition corresponded with the degree of attenuation of target gene expression (Figure 7, Figure 8), suggesting that these genes are essential. The growth inhibition is not caused by GlcN alone, since the growth of the DHS_M9 parasite was unaffected by GlcN treatment. GlcN has no effect on DHS protein expression in the DHS_M9 parasite (Figure 8), as expected since the M9 variant ribozyme carries inactivating mutations at the cleavage site (Winkler et al., 2004). It is generally accepted that DHFR-TS is essential since it is the specific target of antifolate antimalarials (Yuvaniyama et al., 2003). Furthermore, the conclusion of essentiality of the *P. falciparum* DHS gene is in agreement with the inability to knockout this gene in the murine malaria parasite *P. berghei* (Kersting et al., 2016). It is interesting to note that growth inhibition is only obvious after several growth cycles of maximal attenuation of DHS expression (Figure 11). This observation suggests that only a small amount of DHS is needed for growth (less than half the normal level). The robustness of *P. falciparum* to attenuation of expression of other essential genes has been reported, including the PlasmepsinV (Sleebs et al., 2014) and PfATP4 (Ganesan et

al., 2016) genes. We think that the robustness of the parasite to perturbation of gene function is important information for drug development. Robust genes would require high concentrations of specific inhibitors to reduce target gene activity below the threshold needed for parasite viability. Furthermore, drug-resistant parasites would emerge more easily, since variants in robust genes with only a slight reduction in drug affinity would lead to enough functioning target protein for parasite survival. If the *glmS* ribozyme tool could be applied on a genome-wide scale, essential genes could be triaged as drug targets on the basis of their robustness to attenuation. The less robust genes should be accorded higher priority as drug targets, since inhibitory compounds of these targets need not have such high affinities to have high antimalarial potency.

The proof of concept chemogenomic profiling experiments in *P. falciparum* (Figure 12) showed that the primary drug target can be revealed as a significant EC_{50} ratio. All antifolates were identified as DHFR-TS targeting drugs, despite the wide variation in antimalarial potency from the extremely potent WR99210 to PYR in the K1 background, representing a greater than 10^6 difference in EC_{50} value. The test of the K1_ GFP_DHFRTS_*glmS* parasite with PYR showed that even the mutated DHFR-TS in this strain, known to have lower affinity for PYR (Foote et al., 1990); (Yuvaniyama et al., 2003), can still be identified as a PYR target in vivo, albeit with a lower EC_{50} ratio than the PYR-sensitive 3D7_ GFP_DHFRTS_*glmS* parasite. The reason for the lower EC_{50} ratio in the K1_ GFP_DHFRTS_*glmS* parasite is not understood. However, other PYR resistance mechanisms, such as increased *gch1* copy number ((Kidgell et al., 2006); (Nair et al., 2008); (Kumpornsin et al., 2014), may contribute towards the lower EC_{50} ratio. The ability of this chemogenomic profiling approach to identify the primary target is further highlighted by the insignificant EC_{50} ratio for DSM1. This drug is known to target dihydroorotate dehydrogenase (*Pf*DHODH), an enzyme which acts upstream of DHFR-TS in the pyrimidine biosynthetic pathway (Phillips et al., 2008). The chemogenomic approach for identifying targets in vivo can be adapted for high-throughput screening, as shown by our study of the Malaria Box compound library (Spangenberg et al., 2013). The screening data show that attenuation of DHFR-TS has no effect on parasite sensitivity to most of this diverse set of compounds, highlighting the specificity of the approach. A conservative threshold of the EC_{50} ratio (six SDs from the mean) was selected for identifying DHFR-TS targeting compounds, as the method used for estimating the EC_{50} ratio in the screening experiment is likely to have substantial error. High-throughput antimalarial screening procedures can be completed with much smaller volumes (Plouffe et al., 2008); (Gamo et al., 2010); (Guiguemde et al., 2012), such that more data points could be obtained for each compound, leading to more accurate estimate of the EC_{50} ratio and a lower threshold for identifying target-specific compound hits. The compounds MMV667486 and MMV667487, identified from screening as DHFR-TS targeting compounds (Figure 13), possess the antifolate pharmacophore common with CYC, i.e. dihydrotriazine (Yuthavong, 2002). Although the

antifolate pharmacophore is important for interaction with DHFR-TS, it is not sufficient for target specificity in vivo (Plouffe et al., 2008). Chemogenomic profiling therefore provides extra information of target specificity that cannot be predicted from chemical structures alone. Furthermore, it is possible that novel anti-DHFR-TS pharmacophores could be found by chemogenomic profiling of larger and more diverse compound libraries.

Chemogenomic profiling of transgenic parasites with modification of the DHS gene showed that compound N1-guanyl-1,7-diaminoheptane (GC7) targets the DHS gene (Figure 14), as shown by the $\log_2$ EC_{50} (-GlcN/+GlcN) ratio significantly greater than zero for the DHS_*glmS* parasite. In contrast, the $\log_2$ EC_{50} is not significantly different from zero for the control DHS_M9 parasite in which DHS expression is not attenuated by GlcN. Furthermore, $\log_2$ EC_{50} ratios are not significant for the control compounds, i.e. cycloheximide, which targets the ribosome, and pyrimethamine, which targets DHFR-TS. GC7 is described as a potent inhibitor of DHS from different organisms, with an EC_{50} of 17 nM against rat DHS enzyme (Jakus et al., 1993). Given the quite high degree of conservation between rat and *P. falciparum* DHS proteins (62% identity), we assume that compound GC7 is a similarly potent inhibitor of *P. falciparum* DHS. We infer from chemogenomic profiling data that the antimalarial activity of GC7 is due to targeting of *P. falciparum* DHS, and that this gene is essential for parasite growth. Interestingly, the $\log_2$ EC_{50} ratio is only 0.45 for GC7 against the DHS_*glmS* parasite. In comparison, the $\log_2$ EC_{50} ratio is greater than 1.5 for potent antifolate compounds known to bind with high affinity to DHFR-TS (WR99210, MTX, CYC) against the K1_GFP_DHFRTS_*glmS* and 3D7_GFP_DHFRTS_*glmS* parasites (Figure 12). Although these data prove that DHS is the primary *P. falciparum* target of GC7, DHS has rather weak antimalarial activity (EC_{50} of 7 μM in the +GlcN condition for the DHS_*glmS* parasite). Pyrimethamine has similarly weak antimalarial potency to GC7 in the K1 background (EC_{50} of 8 μM in the +GlcN condition for the 1_GFP_DHFRTS_*glmS* parasite). The $\log_2$ EC_{50} ratio is also similarly low (0.81) for pyrimethamine against the K1_GFP_DHFRTS_*glmS* parasite (Figure 12). For less potent antimalarials which bind their targets weakly, we think that inhibition of secondary targets makes a relatively greater contribution to the antimalarial effect compared with potent compounds that bind their primary targets strongly. The inhibition of secondary targets manifests as a lower $\log_2$ EC_{50} ratio, since attenuation of the primary target has less of an impact on the overall antimalarial effect. In target-based drug development, the $\log_2$ EC_{50} ratio may be a useful indicator of target specificity. In a screen of diverse compound libraries, compounds with high $\log_2$ EC_{50} ratios could be triaged as lead compounds for further development.

The validation of DHS as a novel antimalarial target and the identification of two novel DHFR-TS inhibitors from chemogenomic profiling underline the usefulness of the *glmS* reverse genetic tool. The limitation of the tool's ability to attenuate expression up to ten-fold could restrict

the ability to validate robust genes as novel drug targets, since more efficient attenuation of their expression may be needed to observe a growth defect phenotype. It was hypothesized that the *glmS* ribozyme may function more efficiently when positioned in the 5′ UTR, since cleaved target mRNA would lack the 5′ cap, which is critical for RNA stability and translation (Meaux, 2006). The *glmS* ribozyme seems to have a strong inhibitory effect on gene expression when positioned in the 5′ UTR (Figure 15-17). This inhibitory effect could be due to interference of translation initiation (ribosome scanning). The *glmS* ribozyme element has a stable secondary structure (Tinsley et al., 2007), which may inhibit ribosome scanning (Kozak, 2005). Leaky ribozyme activity in the absence of added GlcN could also generate ribozyme-cleaved uncapped RNA. Uncapped mRNA is typically very weakly translated, e.g. as shown with hammerhead ribozyme experiments in yeast (Meaux, 2006). Whatever the reasons for low expression of reporter with *glmS* ribozyme in the 5′ UTR position, it is clear that the strategy of 5′ ribozyme for controlling expression of essential genes may not be useful owing to excessive interference of gene function in the absence of inducer.

In conclusion, the project reached its objectives in identifying a novel antimalarial target (DHS) and establishing a method for identifying antimalarial mode of action.

6. Acknowledgements

We thank the Thailand Research Fund for support of this project. We thank Navaporn Posayapisit, Dr. Chairat Uthaipibull and Dr. Sumalee Kamchonwongpaisan for providing the *Pf*FC_*glmS* transgenic parasite and communicating unpublished data; Ms. Navaporn Posayapisit for screening the Malaria Box compound library and Dr. Taavi Neklesa for providing plasmid pcDNA5-FRT-kozak-HA-EGFP-Halotag2.

7. Output

The primary publications from this work include:

1. Aroonsri A., Akinola O., Posayapisit N., Songsungthong W., Uthaipibull C., Kamchonwongpaisan S., Gbotosho G.O., Yuthavong Y., Shaw P.J. (2016). Identifying antimalarial compounds targeting dihydrofolate reductase-thymidylate synthase (DHFR-TS) by chemogenomic profiling. *Int J Parasitol* ***46***(8):527–535. doi: 10.1016/j.ijpara.2016.04.002

2. Shaw P.J., Aroonsri A. (2017). *Int J Parasitol* (in press, accepted. 30th January, 2017). doi: 10.1016/j.ijpara.2016.11.006.

Secondary publications acknowledging support from the Thailand Research fund:

3. Intarapanich A., Kaewkamnerd S., Pannarut M., Shaw P.J. Tongsima S. (2016). Fast processing of microscopic images using object-based extended depth of field. *BMC Bioinformatics* **17** (Suppl 19):1373. doi: 10.1186/s12859-016-1373-2
4. Posayapisit N., Songsungthong W., Koonyosying P, Falade M.O., Uthaipibull C., Yuthavong Y., Shaw P.J., Kamchonwongpaisan S. (2016). Cytochrome c and c1 heme lyases are essential in *Plasmodium berghei*. *Mol Biochem Parasitol* **210**(1-2):32–36. doi: 10.1016/j.molbiopara.2016.08.003.
5. Shaw P.J., Kaewprommal P., Piriyapongsa J., Wongsombat C., Yuthavong Y., Kamchonwongpaisan S. (2016). Estimating mRNA lengths from *Plasmodium falciparum* genes by virtual northern RNA-seq analysis. *Int J Parasitol* **46**(1):7-12.
6. Intarapanich A., Kaewkamnerd S., Shaw P.J., Ukosakit K., Tragoonrung S.,Tongsima, S. (2015). Automatic DNA diagnosis for 1D gel electrophoresis images using bio-image processing technique. *BMC Genomics* **16**(Suppl 12): S15.
7. Wangkumhang P., Wilantho A., Shaw P.J., Flori L., Moazami-Goudarzi K., Duangjinda M., Assawamakin A., Tongsima S. (2015) Genetic analysis of Thai cattle reveals a Southeast Asian indicine ancestry. *PeerJ* **3**:e1318.
8. Shaw P.J., Chaotheing S., Kaewprommal P., Piriyapongsa J., Wongsombat C., Suwannakitti N., Koonyosying P., Uthaipibull C., Yuthavong Y., Kamchonwongpaisan S. (2015) *Plasmodium* parasites mount an arrest response to dihydroartemisinin, as revealed by whole transcriptome shotgun sequencing (RNA-seq) and microarray study. *BMC Genomics* **16**: 830.

Presentations at meetings:

1. Aroonsri A., Uthaipibull C., Kamchonwongpaisan S., Shaw P.J. Poster presentation titled: "Exploration of essential gene function and anti-malarial mode of action by ribozyme-mediated attenuation of *Plasmodium falciparum* gene activity". 4th Singapore Malaria Network meeting, February 18-19, 2016, Nanyang Executive Centre, Singapore.

2. Pengon, J., Songsungthong, W., Prommana P., Shaw, P.J., Kamchonwongpaisan S., Uthaipibull C. Poster presentation titled: "Screening of 'Malaria box' compounds for their enhanced antimalarial activity in ɣ-glutamylcysteine synthetase-attenuated transgenic *Plasmodium falciparum*". 5th International Biochemistry and Molecular Biology Conference, May 26-27, 2016, B.P. Samila Beach Hotel, Songkhla, Thailand.

3. Aroonsri A., Kongsee J., Thongwichian R., Uthaipibull C., Kamchonwongpaisan S., Shaw, P.J.. Oral presentation titled: "Investigation of deoxyhypusine synthase gene function in *Plasmodium falciparum* using the *glmS* ribozyme reverse genetic tool". 5th International Biochemistry and Molecular Biology Conference, May 26-27, 2016, B.P. Samila Beach Hotel, Songkhla, Thailand.

4. Shaw, P.J. Invited speaker, oral presentation titled: "Application of the *glmS* riboswitch reverse genetic tool in *Plasmodium* spp.". Joint International Tropical Medicine Meeting (JITMM), 7-9 December 2016, Amari Watergate Hotel, Bangkok, Thailand.

5. Posayapisit N., Prommana P., Pengon J., Shaw P.J., Kamchonwongpaisan S., Uthaipibull C. Poster presentation titled: "Identifying Malaria Box compounds targeting dihydrofolate reductase-thymidylate synthase (DHFR-TS)-attenuated transgenic *Plasmodium falciparum*". Keystone Symposia Malaria: From Innovation to Eradication (B5), 19-23 February 2017, Speke Resort & Conference Centre, Kampala, Uganda.

8. Awards

Award for medical science research and development, presented to Philip J. Shaw at the 25th Annual Medical Sciences Conference, Department of Medical Sciences (DMSc) Thailand, IMPACT Forum, Muang Thong Thani, Thailand 22nd – 24th March 2017.

9. Collaborations

The *glmS* ribozyme tool developed by us, and used in this project has been distributed to the following institutes, who have completed Materials Transfer Agreement with the National Science and Technology Development Agency (Thailand) covering the use of the tool.

Burnet Institute, Melbourne Australia

University of Monash, Melbourne, Australia

University of Melbourne, Melbourne, Australia

Australian National University, Canberra, Australia

Pennsylvania State University, Pennsylvania, USA

Deakin University, Victoria, Australia

National Institute of Allergy and Infectious Diseases, Maryland, USA

Ruprecht Karls University of Heidelberg, Heidelberg, Germany

Nagasaki University, Nagasaki, Japan

Walter and Eliza Hall Institute of Medical Research, Melbourne, Australia

University of Georgia Research Foundation, Athens, Georgia, USA

University of Keele, Keele, UK

Leland Stanford University, Stanford, USA

Singapore Immunology Network SIgN, Biomedical Science Institutes, Singapore

National Institute of Immunology (NII), New Delhi, India

Ecole Polytechnique Federale de Lausanne, Lausanne, Switzerland

University of Montpellier, Montpellier, France

Université Laval, Quebec, Canada

National Institute for Medical Research (NIMR), London, UK

Jawaharlal Nehru University, New Delhi, India

International Centre for Genetic Engineering and Biotechnology (ICGEB), New Delhi, India

10. References

Armstrong, C.M., Goldberg, D.E., 2007. An FKBP destabilization domain modulates protein levels in Plasmodium falciparum. Nat. Methods 4, 1007–1009. doi:10.1038/nmeth1132

Aroonsri, A., Akinola, O., Posayapisit, N., Songsungthong, W., Uthaipibull, C., Kamchonwongpaisan, S., Gbotosho, G.O., Yuthavong, Y., Shaw, P.J., 2016. Identifying antimalarial compounds targeting

dihydrofolate reductase-thymidylate synthase (DHFR-TS) by chemogenomic profiling. Int. J. Parasitol. doi:10.1016/j.ijpara.2016.04.002

Aurrecoechea, C., Brestelli, J., Brunk, B.P., Dommer, J., Fischer, S., Gajria, B., Gao, X., Gingle, A., Grant, G., Harb, O.S., Heiges, M., Innamorato, F., Iodice, J., Kissinger, J.C., Kraemer, E., Li, W., Miller, J.A., Nayak, V., Pennington, C., Pinney, D.F., Roos, D.S., Ross, C., Stoeckert, C.J., Treatman, C., Wang, H., 2009. PlasmoDB: a functional genomic database for malaria parasites. Nucleic Acids Res. 37, D539-543. doi:10.1093/nar/gkn814

Azvolinsky, A., Giresi, P.G., Lieb, J.D., Zakian, V.A., 2009. Highly Transcribed RNA Polymerase II Genes Are Impediments to Replication Fork Progression in Saccharomyces cerevisiae. Mol. Cell 34, 722–734. doi:10.1016/j.molcel.2009.05.022

Bates, D., Mächler, M., Bolker, B., Walker, S., 2015. Fitting Linear Mixed-Effects Models Using **lme4**. J. Stat. Softw. 67. doi:10.18637/jss.v067.i01

Baum, J., Papenfuss, A.T., Mair, G.R., Janse, C.J., Vlachou, D., Waters, A.P., Cowman, A.F., Crabb, B.S., de Koning-Ward, T.F., 2009. Molecular genetics and comparative genomics reveal RNAi is not functional in malaria parasites. Nucleic Acids Res. 37, 3788–3798. doi:10.1093/nar/gkp239

Birnbaum, J., Flemming, S., Reichard, N., Soares, A.B., Mesén-Ramírez, P., Jonscher, E., Bergmann, B., Spielmann, T., 2017. A genetic system to study Plasmodium falciparum protein function. Nat. Methods 14, 450–456. doi:10.1038/nmeth.4223

Braks, J.A.M., Franke-Fayard, B., Kroeze, H., Janse, C.J., Waters, A.P., 2006. Development and application of a positive-negative selectable marker system for use in reverse genetics in Plasmodium. Nucleic Acids Res. 34, e39. doi:10.1093/nar/gnj033

Caro, F., Ahyong, V., Betegon, M., DeRisi, J.L., 2014. Genome-wide regulatory dynamics of translation in the *Plasmodium falciparum* asexual blood stages. eLife 3. doi:10.7554/eLife.04106

Cormack, B.P., Valdivia, R.H., Falkow, S., 1996. FACS-optimized mutants of the green fluorescent protein (GFP). Gene 173, 33–38.

Cranmer, S.L., Magowan, C., Liang, J., Coppel, R.L., Cooke, B.M., 1997. An alternative to serum for cultivation of Plasmodium falciparum in vitro. Trans. R. Soc. Trop. Med. Hyg. 91, 363–365. doi:10.1016/S0035-9203(97)90110-3

Crowther, G.J., Shanmugam, D., Carmona, S.J., Doyle, M.A., Hertz-Fowler, C., Berriman, M., Nwaka, S., Ralph, S.A., Roos, D.S., Van Voorhis, W.C., Agüero, F., 2010. Identification of attractive drug targets in neglected-disease pathogens using an in silico approach. PLoS Negl. Trop. Dis. 4, e804. doi:10.1371/journal.pntd.0000804

de Koning-Ward, T.F., Gilson, P.R., Crabb, B.S., 2015. Advances in molecular genetic systems in malaria. Nat. Rev. Microbiol. 13, 373–387. doi:10.1038/nrmicro3450

Deitsch, K., Driskill, C., Wellems, T., 2001. Transformation of malaria parasites by the spontaneous uptake and expression of DNA from human erythrocytes. Nucleic Acids Res. 29, 850–853.

Duraisingh, M.T., Triglia, T., Cowman, A.F., 2002. Negative selection of Plasmodium falciparum reveals targeted gene deletion by double crossover recombination. Int. J. Parasitol. 32, 81–89.

Fatumo, S., Plaimas, K., Adebiyi, E., König, R., 2011. Comparing metabolic network models based on genomic and automatically inferred enzyme information from Plasmodium and its human host to define drug targets in silico. Infect. Genet. Evol. J. Mol. Epidemiol. Evol. Genet. Infect. Dis. 11, 708–715. doi:10.1016/j.meegid.2011.04.013

Fatumo, S., Plaimas, K., Mallm, J.-P., Schramm, G., Adebiyi, E., Oswald, M., Eils, R., König, R., 2009. Estimating novel potential drug targets of Plasmodium falciparum by analysing the metabolic network of knock-out strains in silico. Infect. Genet. Evol. J. Mol. Epidemiol. Evol. Genet. Infect. Dis. 9, 351–358. doi:10.1016/j.meegid.2008.01.007

Feliciello, I., Chinali, G., 1993. A modified alkaline lysis method for the preparation of highly purified plasmid DNA from Escherichia coli. Anal. Biochem. 212, 394–401. doi:10.1006/abio.1993.1346

Fidock, D.A., Wellems, T.E., 1997. Transformation with human dihydrofolate reductase renders malaria parasites insensitive to WR99210 but does not affect the intrinsic activity of proguanil. Proc. Natl. Acad. Sci. U. S. A. 94, 10931–10936.

Flannery, E.L., Chatterjee, A.K., Winzeler, E.A., 2013. Antimalarial drug discovery — approaches and progress towards new medicines. Nat. Rev. Microbiol. 11, 849–862. doi:10.1038/nrmicro3138

Foote, S.J., Galatis, D., Cowman, A.F., 1990. Amino acids in the dihydrofolate reductase-thymidylate synthase gene of Plasmodium falciparum involved in cycloguanil resistance differ from those involved in pyrimethamine resistance. Proc. Natl. Acad. Sci. U. S. A. 87, 3014–3017.

Gamo, F.-J., Sanz, L.M., Vidal, J., de Cozar, C., Alvarez, E., Lavandera, J.-L., Vanderwall, D.E., Green, D.V.S., Kumar, V., Hasan, S., Brown, J.R., Peishoff, C.E., Cardon, L.R., Garcia-Bustos, J.F., 2010. Thousands of chemical starting points for antimalarial lead identification. Nature 465, 305–310. doi:10.1038/nature09107

Ganesan, S.M., Falla, A., Goldfless, S.J., Nasamu, A.S., Niles, J.C., 2016. Synthetic RNA-protein modules integrated with native translation mechanisms to control gene expression in malaria parasites. Nat. Commun. 7, 10727. doi:10.1038/ncomms10727

Ghorbal, M., Gorman, M., Macpherson, C.R., Martins, R.M., Scherf, A., Lopez-Rubio, J.-J., 2014. Genome editing in the human malaria parasite Plasmodium falciparum using the CRISPR-Cas9 system. Nat. Biotechnol. 32, 819–821. doi:10.1038/nbt.2925

Gibson, D.G., Young, L., Chuang, R.-Y., Venter, J.C., Hutchison, C.A., Smith, H.O., 2009. Enzymatic assembly of DNA molecules up to several hundred kilobases. Nat. Methods 6, 343–345. doi:10.1038/nmeth.1318

Guiguemde, W.A., Shelat, A.A., Garcia-Bustos, J.F., Diagana, T.T., Gamo, F.-J., Guy, R.K., 2012. Global Phenotypic Screening for Antimalarials. Chem. Biol. 19, 116–129. doi:10.1016/j.chembiol.2012.01.004

Herberich, E., Sikorski, J., Hothorn, T., 2010. A Robust Procedure for Comparing Multiple Means under Heteroscedasticity in Unbalanced Designs. PLoS ONE 5, e9788. doi:10.1371/journal.pone.0009788

Huthmacher, C., Hoppe, A., Bulik, S., Holzhütter, H.-G., 2010. Antimalarial drug targets in Plasmodium falciparum predicted by stage-specific metabolic network analysis. BMC Syst. Biol. 4, 120.

Imwong, M., Suwannasin, K., Kunasol, C., Sutawong, K., Mayxay, M., Rekol, H., Smithuis, F.M., Hlaing, T.M., Tun, K.M., van der Pluijm, R.W., Tripura, R., Miotto, O., Menard, D., Dhorda, M., Day, N.P.J., White, N.J., Dondorp, A.M., 2017. The spread of artemisinin-resistant Plasmodium falciparum in the Greater Mekong subregion: a molecular epidemiology observational study. Lancet Infect. Dis. 17, 491–497. doi:10.1016/S1473-3099(17)30048-8

Ito, D., Schureck, M.A., Desai, S.A., 2017. An essential dual-function complex mediates erythrocyte invasion and channel-mediated nutrient uptake in malaria parasites. eLife 6. doi:10.7554/eLife.23485

Jakus, J., Wolff, E.C., Park, M.H., Folk, J.E., 1993. Features of the spermidine-binding site of deoxyhypusine synthase as derived from inhibition studies. Effective inhibition by bis- and mono-guanylated diamines and polyamines. J. Biol. Chem. 268, 13151–13159.

Ke, H., Sigala, P.A., Miura, K., Morrisey, J.M., Mather, M.W., Crowley, J.R., Henderson, J.P., Goldberg, D.E., Long, C.A., Vaidya, A.B., 2014. The heme biosynthesis pathway is essential for Plasmodium falciparum development in mosquito stage but not in blood stages. J. Biol. Chem. 289, 34827–34837. doi:10.1074/jbc.M114.615831

Kersting, D., Krüger, M., Sattler, J.M., Mueller, A.-K., Kaiser, A., 2016. A suggested vital function for eIF-5A and dhs genes during murine malaria blood-stage infection. FEBS Open Bio 6, 860–872. doi:10.1002/2211-5463.12093

Kidgell, C., Volkman, S.K., Daily, J., Borevitz, J.O., Plouffe, D., Zhou, Y., Johnson, J.R., Le Roch, K.G., Sarr, O., Ndir, O., Mboup, S., Batalov, S., Wirth, D.F., Winzeler, E.A., 2006. A Systematic Map of Genetic Variation in Plasmodium falciparum. PLoS Pathog. 2, e57. doi:10.1371/journal.ppat.0020057

Kozak, M., 2005. Regulation of translation via mRNA structure in prokaryotes and eukaryotes. Gene 361, 13–37. doi:10.1016/j.gene.2005.06.037

Kumpornsin, K., Modchang, C., Heinberg, A., Ekland, E.H., Jirawatcharadech, P., Chobson, P., Suwanakitti, N., Chaotheing, S., Wilairat, P., Deitsch, K.W., Kamchonwongpaisan, S., Fidock, D.A., Kirkman, L.A., Yuthavong, Y., Chookajorn, T., 2014. Origin of Robustness in Generating Drug-Resistant Malaria Parasites. Mol. Biol. Evol. 31, 1649–1660. doi:10.1093/molbev/msu140

Lambros, C., Vanderberg, J.P., 1979. Synchronization of Plasmodium falciparum erythrocytic stages in culture. J. Parasitol. 65, 418–420.

Ludin, P., Woodcroft, B., Ralph, S.A., Mäser, P., 2012. In silico prediction of antimalarial drug target candidates. Int. J. Parasitol. Drugs Drug Resist. 2, 191–199. doi:10.1016/j.ijpddr.2012.07.002

McCown, P.J., Roth, A., Breaker, R.R., 2011. An expanded collection and refined consensus model of glmS ribozymes. RNA N. Y. N 17, 728–736. doi:10.1261/rna.2590811

Meaux, S., 2006. Yeast transcripts cleaved by an internal ribozyme provide new insight into the role of the cap and poly(A) tail in translation and mRNA decay. RNA 12, 1323–1337. doi:10.1261/rna.46306

Muralidharan, V., Oksman, A., Iwamoto, M., Wandless, T.J., Goldberg, D.E., 2011. Asparagine repeat function in a Plasmodium falciparum protein assessed via a regulatable fluorescent affinity tag. Proc. Natl. Acad. Sci. 108, 4411–4416. doi:10.1073/pnas.1018449108

Nair, S., Miller, B., Barends, M., Jaidee, A., Patel, J., Mayxay, M., Newton, P., Nosten, F., Ferdig, M.T., Anderson, T.J.C., 2008. Adaptive Copy Number Evolution in Malaria Parasites. PLoS Genet. 4, e1000243. doi:10.1371/journal.pgen.1000243

Neklesa, T.K., Tae, H.S., Schneekloth, A.R., Stulberg, M.J., Corson, T.W., Sundberg, T.B., Raina, K., Holley, S.A., Crews, C.M., 2011. Small-molecule hydrophobic tagging–induced degradation of HaloTag fusion proteins. Nat. Chem. Biol. 7, 538–543. doi:10.1038/nchembio.597

Nijman, S.M.B., 2015. Functional genomics to uncover drug mechanism of action. Nat. Chem. Biol. 11, 942–948. doi:10.1038/nchembio.1963

Phillips, M.A., Gujjar, R., Malmquist, N.A., White, J., El Mazouni, F., Baldwin, J., Rathod, P.K., 2008. Triazolopyrimidine-Based Dihydroorotate Dehydrogenase Inhibitors with Potent and Selective Activity against the Malaria Parasite *Plasmodium falciparum*. J. Med. Chem. 51, 3649–3653. doi:10.1021/jm8001026

Plata, G., Hsiao, T.-L., Olszewski, K.L., Llinás, M., Vitkup, D., 2010. Reconstruction and flux-balance analysis of the Plasmodium falciparum metabolic network. Mol. Syst. Biol. 6, 408. doi:10.1038/msb.2010.60

Plouffe, D., Brinker, A., McNamara, C., Henson, K., Kato, N., Kuhen, K., Nagle, A., Adrián, F., Matzen, J.T., Anderson, P., Nam, T., Gray, N.S., Chatterjee, A., Janes, J., Yan, S.F., Trager, R., Caldwell, J.S., Schultz, P.G., Zhou, Y., Winzeler, E.A., 2008. *In silico* activity profiling reveals the mechanism of action of antimalarials discovered in a high-throughput screen. Proc. Natl. Acad. Sci. 105, 9059–9064. doi:10.1073/pnas.0802982105

Prommana, P., Uthaipibull, C., Wongsombat, C., Kamchonwongpaisan, S., Yuthavong, Y., Knuepfer, E., Holder, A.A., Shaw, P.J., 2013. Inducible Knockdown of Plasmodium Gene Expression Using the glmS Ribozyme. PLoS ONE 8, e73783. doi:10.1371/journal.pone.0073783

Raveendranathan, M., Chattopadhyay, S., Bolon, Y.-T., Haworth, J., Clarke, D.J., Bielinsky, A.-K., 2006. Genome-wide replication profiles of S-phase checkpoint mutants reveal fragile sites in yeast. EMBO J. 25, 3627–3639. doi:10.1038/sj.emboj.7601251

Ritz, C., Streibig, J.C., 2005. Bioassay analysis using R. J. Stat. Softw. 12, 1–22.

Schembri, L., Dalibart, R., Tomasello, F., Legembre, P., Ichas, F., De Giorgi, F., 2007. The HA tag is cleaved and loses immunoreactivity during apoptosis. Nat. Methods 4, 107–108. doi:10.1038/nmeth0207-107

Schneider, C.A., Rasband, W.S., Eliceiri, K.W., 2012. NIH Image to ImageJ: 25 years of image analysis. Nat. Methods 9, 671–675.

Shaw, P.J., Aroonsri, A., 2017. Tools for attenuation of gene expression in malaria parasites. Int. J. Parasitol. doi:10.1016/j.ijpara.2016.11.006

Sigala, P.A., Crowley, J.R., Henderson, J.P., Goldberg, D.E., 2015. Deconvoluting heme biosynthesis to target blood-stage malaria parasites. eLife 4. doi:10.7554/eLife.09143

Sleebs, B.E., Lopaticki, S., Marapana, D.S., O'Neill, M.T., Rajasekaran, P., Gazdik, M., Günther, S., Whitehead, L.W., Lowes, K.N., Barfod, L., Hviid, L., Shaw, P.J., Hodder, A.N., Smith, B.J., Cowman, A.F., Boddey, J.A., 2014. Inhibition of Plasmepsin V Activity Demonstrates Its Essential Role in Protein Export, PfEMP1 Display, and Survival of Malaria Parasites. PLoS Biol. 12, e1001897. doi:10.1371/journal.pbio.1001897

Smilkstein, M., Sriwilaijaroen, N., Kelly, J.X., Wilairat, P., Riscoe, M., 2004. Simple and inexpensive fluorescence-based technique for high-throughput antimalarial drug screening. Antimicrob. Agents Chemother. 48, 1803–1806.

Song, W., Dominska, M., Greenwell, P.W., Petes, T.D., 2014. Genome-wide high-resolution mapping of chromosome fragile sites in Saccharomyces cerevisiae. Proc. Natl. Acad. Sci. 111, E2210–E2218. doi:10.1073/pnas.1406847111

Spangenberg, T., Burrows, J.N., Kowalczyk, P., McDonald, S., Wells, T.N.C., Willis, P., 2013. The open access malaria box: a drug discovery catalyst for neglected diseases. PloS One 8, e62906. doi:10.1371/journal.pone.0062906

Tanner, M., Greenwood, B., Whitty, C.J.M., Ansah, E.K., Price, R.N., Dondorp, A.M., von Seidlein, L., Baird, J.K., Beeson, J.G., Fowkes, F.J.I., Hemingway, J., Marsh, K., Osier, F., 2015. Malaria eradication and elimination: views on how to translate a vision into reality. BMC Med. 13. doi:10.1186/s12916-015-0384-6

Tinsley, R.A., Furchak, J.R.W., Walter, N.G., 2007. Trans-acting glmS catalytic riboswitch: locked and loaded. RNA N. Y. N 13, 468–477. doi:10.1261/rna.341807

Trager, W., Jensen, J.B., 1976. Human malaria parasites in continuous culture. Science 193, 673–675.

Vaughan, A.M., O'Neill, M.T., Tarun, A.S., Camargo, N., Phuong, T.M., Aly, A.S.I., Cowman, A.F., Kappe, S.H.I., 2009. Type II fatty acid synthesis is essential only for malaria parasite late liver stage development. Cell. Microbiol. 11, 506–20. doi:10.1111/j.1462-5822.2008.01270.x

Waterkeyn, J.., Crabb, B.., Cowman, A.., 1999. Transfection of the human malaria parasite Plasmodium falciparum. Int. J. Parasitol. 29, 945–955. doi:10.1016/S0020-7519(99)00047-8

Winkler, W.C., Nahvi, A., Roth, A., Collins, J.A., Breaker, R.R., 2004. Control of gene expression by a natural metabolite-responsive ribozyme. Nature 428, 281–286.

Wu, Y., Sifri, C.D., Lei, H.H., Su, X.Z., Wellems, T.E., 1995. Transfection of Plasmodium falciparum within human red blood cells. Proc. Natl. Acad. Sci. U. S. A. 92, 973–977.

Yadav, M.K., Pandey, S.K., Swati, D., 2013. DRUG TARGET PRIORITIZATION IN *PLASMODIUM FALCIPARUM* THROUGH METABOLIC NETWORK ANALYSIS, AND INHIBITOR DESIGNING USING VIRTUAL SCREENING AND DOCKING APPROACH. J. Bioinform. Comput. Biol. 11, 1350003. doi:10.1142/S0219720013500030

Yeh, I., Hanekamp, T., Tsoka, S., Karp, P.D., Altman, R.B., 2004. Computational analysis of Plasmodium falciparum metabolism: organizing genomic information to facilitate drug discovery. Genome Res. 14, 917–924. doi:10.1101/gr.2050304

Yuan, L., Hao, M., Wu, L., Zhao, Z., Rosenthal, B.M., Li, X., He, Y., Sun, L., Feng, G., Xiang, Z., Cui, L., Yang, Z., 2014. Refrigeration provides a simple means to synchronize in vitro cultures of Plasmodium falciparum. Exp. Parasitol. 140, 18–23. doi:10.1016/j.exppara.2014.03.010

Yuthavong, Y., 2002. Basis for antifolate action and resistance in malaria. Microbes Infect. Inst. Pasteur 4, 175–182.

Yuthavong, Y., Tarnchompoo, B., Vilaivan, T., Chitnumsub, P., Kamchonwongpaisan, S., Charman, S.A., McLennan, D.N., White, K.L., Vivas, L., Bongard, E., others, 2012. Malarial dihydrofolate reductase as a paradigm for drug development against a resistance-compromised target. Proc. Natl. Acad. Sci. 109, 16823–16828.

Yuvaniyama, J., Chitnumsub, P., Kamchonwongpaisan, S., Vanichtanankul, J., Sirawaraporn, W., Taylor, P., Walkinshaw, M.D., Yuthavong, Y., 2003. Insights into antifolate resistance from malarial DHFR-TS structures. Nat. Struct. Biol. 10, 357–365. doi:10.1038/nsb921

11. Appendix: reprints of published output